Irrgeher, J.; Galler, P.; Prohaska, T.:

87Sr/86Sr isotope ratio measurements by laser ablation multicollector inductively coupled plasma mass spectrometry: Reconsidering matrix interferences in bioapatites and biogenic carbonates

In: Spectrochimica Acta B (2016) Elsevier

DOI: 10.1016/j.sab.2016.09.008

$^{87}Sr/^{86}Sr$ isotope ratio measurements by laser ablation multicollector inductively coupled plasma mass spectrometry: reconsidering matrix interferences in bioapatites and biogenic carbonates

Johanna Irrgeher[a*§], Patrick Galler[b] and Thomas Prohaska[a]

[a] University of Natural Resources and Life Sciences Vienna, Department of Chemistry, Division of Analytical Chemistry, VIRIS Laboratory, Konrad-Lorenz-Strasse 24, 3430 Tulln, Austria

[b] Elkem Technology - Lab projects, Fiskaavn. 100, P.O. Box 8040 Vaagsbygd, NO-4675 Kristiansand S., Norway

*Affiliation when the research was performed; present address: Helmholtz-Centre for Materials and Coastal Research, Institute for Coastal Research, Department for Marine Bioanalytical Chemistry, Max-Planck-Straße 1, 21502 Geesthacht, Germany

[$] corresponding author: johanna Irrgeher@hzg.de

ABSTRACT

This study is dedicated to the systematic investigation of the effect of interferences on Sr isotopic analyses in biological apatite and carbonate matrices using laser ablation multicollector inductively coupled plasma mass spectrometry (LA-MC ICP-MS). Trends towards higher $^{87}Sr/^{86}Sr$ ratios for LA-MC ICP-MS compared to solution-nebulization based MC ICP-MS when analyzing bioapatite matrices (e.g. human teeth) and lower ratios in case of calcium carbonates (e.g. fish earstones) were observed. This effect can be related to the presence of significant matrix-related interferences such as molecular ions (e.g. $(^{40}Ca\text{-}^{31}P\text{-}^{16}O)^+$, $(^{40}Ar\text{-}^{31}P\text{-}^{16}O)^+$, $(^{42}Ca\text{-}^{44}Ca)^+$, $(^{46}Ca^{40}Ar)^+$) as well as in many cases concomitant atomic ions (e.g. $^{87}Rb^+$, $^{174}Hf^{2+}$). Direct $^{87}Sr/^{86}Sr$ ratio measurements in Ca-rich samples are conducted without the possibility of prior sample separation, which can be accomplished routinely for solution-based analysis. The presence of Ca-Ar and Ca-Ca molecular ion interferences in the mass range of Sr isotopes is shown using the mass resolving capabilities of a single collector inductively coupled plasma sector field mass spectrometer operated in medium mass resolution when analysing bioapatites and calcium carbonate samples.

The major focus was set on analysing human tooth samples, fish hard parts and geological carbonates. Potential sources of interferences were identified and corrected for. The combined corrections of interferences and adequate instrumental isotopic fractionation correction procedures lead to accurate data even though increased uncertainties have to be taken into account. The results are discussed along with approaches presented in literature for data correction in laser ablation analysis.

Keywords: strontium isotope ratios, bioapatite, biogenic calcium carbonate, laser ablation, interferences, MC ICP-MS

1 INTRODUCTION

Sr isotope ratio analysis in both human and animal hard tissues can give insight into diverse present as well as past ecological questions and thus has become an indispensable means in different research disciplines such as ecogeochemistry, geochemistry and forensics to address e.g. anthropological and archaeological as well as hydrobiological research issues [1] [2] [3] [4]. As a consequence $^{87}Sr/^{86}Sr$ isotope ratios in biological apatites and calcium carbonates have been assessed for decades as a powerful tool for tracing migration and mobility phenomena. Today, both thermal ionisation mass spectrometry (TIMS) and solution-based multicollector inductively coupled

plasma mass spectrometry (MC ICP-MS) can be considered as benchmark methods in Sr isotope ratio measurements [5, 6].

Sr isotope ratio analysis of archaeological relicts such as human tooth and bone has most frequently been accomplished by mechanically sampling fractions of sample material followed by acid digestion, Sr/matrix separation and final measurement using solution-based MC ICP-MS [7] [8] [9] [10] [5] [6] [4]. Even though this analytical approach allows for accurate Sr isotope ratios comparable to TIMS data, laser ablation multicollector inductively coupled plasma mass spectrometry (LA-MC ICP-MS) offers great advantages over these well-established methodologies, however suffering from poorer measurement precision. The technique stands out due to its attributes as a semi-invasive means for the fast and direct investigation of Sr isotope ratios, marginal sample preparation required and the possibility of solid sample analyses at small scales. The latter has become a key issue considering the growth characteristics of favoured samples investigated such as human teeth or fish hard parts. These matrices continuously grow in increments or layers and therefore record chemical information at small scales (< 100 µm), including time-dependent variation in the isotopic composition of incorporated Sr. Undoubtedly, assessing this information is highly desirable.

Around the turn of the millennium, first results using laser ablation as sampling approach for Sr isotope ratio measurements by (MC) ICP-MS were deemed to be promising, even though some of these measurements were accomplished using single collector instruments. Moreover, the potential influence of interferences was not investigated in detail [9, 11]. In the course of time, the advent of instrumentation with improved measurement precision has continuously triggered improvement for corrections of blank, instrumental isotopic fractionation and putative interferences. As a consequence aspects such as natural fractionation of stable Sr isotopes, mass-dependent as well as mass-independent instrumental isotopic fractionation and the parallel use of different absolute $^{88}Sr/^{86}Sr$ reference values used for corrections have to be studied in detail and considered when Sr isotope ratios are assessed [12]. This is of particular importance since conventional Sr isotope ratio measurements apply instrumental isotopic fractionation corrections following an internal correction approach for correcting the $^{87}Sr/^{86}Sr$ isotope ratio using the $^{88}Sr/^{86}Sr$ ratio in the same sample. In this approach the $^{88}Sr/^{86}Sr$ ratio is assumed to be invariant in nature. However, this strategy is to be reconsidered since the $^{88}Sr/^{86}Sr$ isotope ratio was shown to vary significantly in natural samples [13] [14] [15]. The reported variation of $\delta(^{88}Sr/^{86}Sr)$ ranges from –1.06 ± 0.02 to + 1.373 ± 0.007 ‰, even though most published values lie between 0.1 and 0.5 ‰ [16].

Table 1

Selected major interferences to be considered in the mass range 82 – 88, given with their natural abundances and the mass resolution (m/z)/$\Delta(m/z)$ required to separate the interference from the analyte (according to the 10 % mass valley definition).

m/z	82		83		**84**		85		**86**		**87**		**88**	
analyte	$^{82}Kr^+$	*11.59 %*	$^{83}Kr^+$	*11.50 %*	$^{84}Sr^+$	***0.56 %***	$^{85}Rb^+$	*72.17 %*	$^{86}Sr^+$	***9.86 %***	$^{87}Sr^+$	***7.00 %***	$^{88}Sr^+$	***82.58 %***
(m/z)/Δ(m/z)	$^{42}Ca\,^{40}Ar^+$	*0.644*	$^{43}Ca\,^{40}Ar^+$	*0.14*	$^{84}Kr^+$	*56.987*	$^{42}Ca\,^{43}Ca^+$	*0.001*	$^{86}Kr^+$	*17.279*	$^{87}Rb^+$	*27.83*	$^{44}Ca\,^{44}Ca^+$	*0.044*
> 10000	$^{42}Ca\,^{40}Ca^+$	*0.627*	$^{82}Kr\,^{1}H^+$	*11.6*	$^{46}Ca\,^{38}Ar^+$	*0.000003*			$^{42}Ca\,^{44}Ca^+$	*0.013*	$^{43}Ca\,^{44}Ca^+$	*0.003*	$^{46}Ca\,^{42}Ca^+$	*0.00003*
			$^{43}Ca\,^{40}Ca^+$	*0.13*	$^{44}Ca\,^{40}Ca^+$	*1.026*			$^{48}Ca\,^{38}Ar^+$	*0.0001*				
					$^{42}Ca\,^{42}Ca^+$	*0.004*			$^{46}Ca\,^{40}Ar^+$	*0.004*				
					$^{44}Ca\,^{40}Ar^+$	*1.055*			$^{40}Ca\,^{46}Ca^+$	*0.004*				
									$^{43}Ca\,^{43}Ca^+$	*0.003*				
(m/z)/Δ(m/z)	$^{80}Kr\,^{2}H^+$	*0.001*			$^{48}Ca\,^{36}Ar^+$	*0.001*	$^{48}Ca\,^{36}Ar\,^{1}H^+$	*0.001*					$^{48}Ca\,^{40}Ca^+$	*0.181*
4000-10000	$^{80}Kr(^{1}H)_2^+$	*2.25*			$^{44}Ca\,^{38}Ar\,^{2}H^+$	*0.02*	$^{46}Ca\,^{38}Ar\,^{1}H^+$	*0.000003*					$^{48}Ca\,^{40}Ar^+$	*0.186*
	$^{42}Ca\,^{38}Ar\,^{2}H^+$	*0.0000001*					$^{44}Ca\,^{40}Ar\,^{1}H^+$	*0.007*						
	$^{44}Ca\,^{36}Ar\,^{2}H^+$	*0.000001*												
(m/z)/Δ(m/z)	$^{40}Ar\,^{40}Ar\,^{2}H^+$	*0.02*	$^{36}Ar\,^{31}P\,^{16}O^+$	*0.336*	$^{42}Ca\,^{40}Ar\,^{2}H^+$	*0.01*	$^{38}Ar\,^{31}P\,^{16}O^+$	*0.063*	$^{172}Yb^{++}$	*21.83*	$^{40}Ar\,^{31}P\,^{16}O^+$	*99.361*	$^{36}Ar\,^{36}Ar\,^{16}O^+$	*0.001*
> 400	$^{40}Ca\,^{40}Ar\,^{2}H^+$	*1.93*	$^{166}Er^{2+}$	*33.503*	$^{168}Er^{2+}$	*26.978*	$^{43}Ca\,^{40}Ca\,^{2}H^+$	*0.00003*			$^{40}Ca\,^{31}P\,^{16}O^+$	*96.708*	$^{16}O(^{36}Ar)_2^+$	*0.001*
	$^{48}Ca\,^{18}O\,^{16}O^+$	*0.0004*			$^{168}Yb^{2+}$	*0.13*	$^{36}Ar\,^{31}P\,^{18}O^+$	*0.001*			$^{38}Ar\,^{31}P\,^{18}O^+$	*0.0001*	$^{40}Ar\,^{31}P\,^{17}O^+$	*0.039*
	$^{46}Ca(^{18}O)_2^+$	*0.00000002*					$^{170}Yb^{2+}$	*3.04*			$^{174}Yb^{2+}$	*31.83*	$^{176}Yb^{2+}$	*12.76*
	$^{164}Dy^{2+}$	*28.18*					$^{170}Er^{2+}$	*14.91*			$^{174}Hf^{2+}$	*0.16*	$^{176}Lu^{2+}$	*2.59*
	$^{164}Er^{2+}$	*1.601*											$^{176}Hf^{2+}$	*5.26*

Interferences on Sr isotopes analysed by LA-MC ICP-MS have been subject to numerous debates and discussions in the field during the last couple of years, as diverse sources of interferences are presumed and corrections are approached differently. Mostly, trends towards higher $^{87}Sr/^{86}Sr$ are reported for LA-MC ICP-MS compared to solution-nebulisation based MC ICP-MS when analysing apatite matrices and lower ratios in case of $CaCO_3$ samples [17] [18] [19] [20] [21] [22]. Table 1 gives an overview of matrix-based interferences in the mass range of 82 – 88 and the required mass resolution required separating the interference from the analyte (according to the 10 % mass valley definition). A great number of these interferences cannot be resolved in low mass resolution (i.e. $(m/z)/\Delta(m/z) < 300$). Abundances of molecular species were calculated based on the assumption that all isotope combinations of e.g. Ar and Ca sum up to 100 %.

Woodhead et al. (2005)[23] were among the first to point out the necessity of correcting for Ca-Ar interferences and Ca-dimers when analysing carbonate matrices, reporting higher $^{87}Sr/^{86}Sr$ ratios for TIMS measurements compared to LA-MC ICP-MS. The authors monitored the $(^{42}Ca^{40}Ar)^+$ and $(^{42}Ca^{40}Ca)^+$ peak at m/z 82 and subsequently corrected for the contributions at m/z 84, 86 and 88. The authors discussed further the presence of interfering doubly charged rare earth elements (REEs). The relevance of REEs was considered negligible in their study on modern carbonates at that time. Since then, Sr isotope ratio measurements in Ca-rich matrices using LA-MC ICP-MS have been systematically investigated by a number of researchers. A selection of different studies is given in Table 2. Recently, Yang *et al*. presented a correction strategy for inferences caused by doubly charged REE (rare earth element) ions [24]. In another recent study, the significance of Ca-based interferences was shown negligible [25]. Also, the potential of tandem ICP-MS for Sr isotopic analysis without prior Rb/Sr separation was shown [26].

The remarkable number of publications clearly shows that Sr isotope ratio analyses by LA-MC ICP-MS remains a challenging task as the presence and significance of interferences are understood in different ways. Therefore, this topic demands further investigations to enable reliable data treatment before sound interpretations in any research field can be performed.

Table 2
Selected publications about Sr isotope ratio analysis by LA-MC ICP-MS since 1995 – experimental setups and data evaluation strategies.

experimental setup						data evaluation strategies (as stated by the authors)						
reference	MC ICP-MS	laser system	LA gas	add. sample introduction	analyzed matrices	blank / Kr	Rb	Ca dimer/argide	Ca-P-O, Ar-P-O	REE	IIF	other
Christensen et al. 1995 [11]	VG P54	Nd:YAG (266 nm) /Laser probe built by Fisons	Ar	-	feldspar, modern shell	^{83}n/a / ^{83}Kr peak stripping	^{85}Rb peak stripping ($f_{Rb} = f_{Sr}$)	-	-	-	internal via $^{88}Sr/^{86}Sr$	-
Outridge et al. 2002 [27]	VG P54	VG Microprobe 2 (266 nm)	Ar	Ar via Cetac MCN 6000 desolv. membrane	fish otoliths	zero point correction at 0.5 amu from peak, [n/a Kr]	^{85}Rb peak stripping ($f_{Rb} = f_{Sr}$)	-	-	-	no IIF correction	-
Bizzarro et al. 2002 [28]	IsoProbe (Micromass)	193nm ArF excimer /Compex 102 - Lambda Physik	He	Ar via Y-piece to Aridus microconcentric nebulizer	apatite, carbonate	gas blank	^{85}Rb peak stripping ($f_{Rb} = f_{Sr}$)	monitored via invariant $^{84}Sr/^{88}Sr$, $^{84}Sr/^{86}Sr$	-	monitored via invariant $^{84}Sr/^{88}Sr$, $^{84}Sr/^{86}Sr$	internal via $^{88}Sr/^{86}Sr$	FeO_2 monitored via invariant $^{84}Sr/^{88}Sr$, $^{84}Sr/^{86}Sr$
Woodhead et al. 2004 [23]	Nu Plasma (Nu Instruments)	HelEx 193 nm ArF excimer; Lambda Physik Compex	He	mixed with Ar carrier gas	modern carbonates	gas blank/ on-peak	^{85}Rb peak stripping ($f_{Rb} = f_{Sr}$)	correction via mass 82	-	not relevant in modern carbonates, ^{89}Y monitored as REE proxy	internal via $^{88}Sr/^{86}Sr$	-
Jackson and Hart 2006 [29]	Thermo-Finnigan Neptune	NewWave UP213nm	He	mixed with 5% HNO_3	basalt glasses	baseline of 0.7 amu defocused beam, subtracting ^{84}Kr until $^{84}Sr/^{86}Sr$ = 0.0565725	standard bracketing with TIMS characterized basalt glass	-	-	correction of REEs by monitoring $^{171}Yb^{++}$ and $^{167}Er^{++}$	internal via $^{88}Sr/^{86}Sr$	correction strategies underway for FeO_2, KrH, Ca dimers/argides
Simonetti et al. 2007 [30]	Nu Plasma (Nu Instruments)	Nd:YAG UP213nm	He	mixed with 2% HNO_3 via DSN-100	historic human tooth enamel	n/a	^{85}Rb peak stripping ($f_{Rb} = f_{Sr}$)	-	observation of Ca-P-O using ICPQMS	n/a	n/a	-
Horstwood et al. 2008 [18]	Nu Plasma (Nu Instruments)	New Wave UP193SS Nd:YAG 193nm	He	-	tooth enamel, apatite, modern mollusc shell	on-peak-zero, gas blank	^{85}Rb peak stripping ($f_{Rb} \neq f_{Sr}$), 'true' $^{85}Rb/^{87}Rb$ ratio determined by standard analysis	correction for $^{40}Ca^{44}Ca$, $^{40}Ca^{46}Ca$ via monitoring of $^{40}Ca^{42}Ca$	calibration against TIMS characterized samples and correction of Ca-P-O	correction for $^{163}Dy^{2+}$, $^{167}Er^{2+}$, $^{175}Lu^{2+}$, $^{171}Yb^{2+}$ and $^{173}Yb^{2+}$ via monitoring at half-masses	internal via $^{88}Sr/^{86}Sr$	-
Richards et al. 2008 [19]	Thermo-Finnigan Neptune	NewWave UP213nm	Ar + He	-	neanderthal, rhino, deer teeth	n/a	n/a	n/a	n/a	n/a	n/a	correction of LA data by a constant subtrahend of 0.001 established by TIMS
Copeland et al. 2008 [17]	Nu Plasma (Nu Instruments)	NewWave UP213nm	He	Ar via Y-piece	modern rodent teeth	on-peak gas blank	^{85}Rb peak stripping ($f_{Rb} = f_{Sr}$)	monitored via invariant $^{84}Sr/^{86}Sr$; no significant effect present	no significant effect present	-	internal via $^{88}Sr/^{86}Sr$	

Copeland et al. 2010 [22]	Nu Plasma (Nu Instruments)	NewWave UP213nm	He	Ar via Y-piece	fossil teeth	on-peak gas blank	^{85}Rb peak stripping ($f_{Rb} = f_{Sr}$)	correction via mass 82	no significant effect present	correction of REEs by monitoring $^{173}Yb^{++}$ and $^{166}Er^{++}$	internal via $^{88}Sr/^{86}Sr$	
Yang et al. 2011 [31]	Thermo-Finnigan Neptune	fs-LA system (785nm) (Quantronix, USA)	Ar	-	otolith RM, igneous fluorite	gas blank	^{85}Rb peak stripping ($f_{Rb} = f_{Sr}$)	considered as negligible based on systematic investigations	n/a	$^{172}Yb^{++}$, $^{176}Yb^{++}$, $^{176}Lu^{++}$, $^{168}Er^{++}$, $^{168}Yb^{++}$, $^{170}Er^{++}$, $^{170}Yb^{++}$, $^{174}Yb^{++}$ via monitoring $^{167}Er^{++}$ and $^{172}Yb^{++}$ on 83.5 and 86.5	internal via $^{88}Sr/^{86}Sr$	
Wu et al. 2010 [32]	Thermo-Finnigan Neptune	ArF excimer laser (Geolas CQ)	He	-	eudialyte	gas blank, ^{83}Kr peak stripping	^{85}Rb peak stripping ($f_{Rb} = f_{Sr}$)	considered as negligible	n/a	correction of REEs by monitoring $^{173}Yb^{++}$, $^{171}Yb^{++}$ and $^{167}Er^{++}$, no corrections for $^{176}Hf^{++}$ and $^{176}Lu^{++}$ (low signal intensities observed)	n/a	

2 EXPERIMENTAL

2.1 Materials, reagents and standards

All preparative laboratory work was performed in a class 100 000 clean room. HNO_3 was prepared by double subboiling distillation (Milestone-MLS GmbH, Leutkirch, Germany) of analytical reagent grade acid (Merck KGaA, Darmstadt, Germany). Reagent grade type I water (18 MΩ cm) (F+L GmbH, Vienna, Austria) was further purified by subboiling distillation (Milestone-MLS GmbH).

NIST SRM 987 $SrCO_3$ with a certified isotopic composition of $^{87}Sr/^{86}Sr = 0.71034 \pm 0.00026$, NIST SRM 984 RbCl with a certified isotopic composition of $^{85}Rb/^{87}Rb = 2.538 \pm 0.002$, NIST SRM 1400 bone ash and NIST SRM 1486 bone meal with certified Sr concentrations of 249 ± 7 μg g^{-1} and 264 ± 7 μg g^{-1} respectively, were used for quality control (all standards from: National Institute of Standards and Technology, Gaithersburg, USA). Commercially available high-purity polyethylene powder (PE) (Sigma Aldrich, St. Louis, USA), hydroxyapatite [$Ca_{10}(PO_4)_6(OH)_2$] (Sigma Aldrich) as well as $CaCO_3$ (p.a., precipitated, Merck) were used for preparation of solid quality control samples. A single element Zr concentration standard (1000 ppm Zirconium for ICP, Inorganic Ventures, Christiansburg, USA) was used for instrumental isotopic fractionation studies.

2.2 Samples

2.2.1 Biological apatite samples

Two commercially available bone reference materials (NIST SRM 1400 bone ash and NIST SRM 1486 bone meal) were analysed for their $^{87}Sr/^{86}Sr$ isotope ratios over long-term periods [33] [34]. For preparation of the actual laser ablation targets NIST SRM 1400 bone ash and NIST SRM 1486 bone meal were mixed with high purity poly-ethylene (PE) and pressed into pellets by means of a conventional laboratory press at a pressure of 8 tons applied for 5 – 7 minutes, using stainless steel plungers. The $^{87}Sr/^{86}Sr$ ratio of the solid standards was determined by LA-MC ICP-MS as well as by liquid based MC ICP-MS (after Sr/matrix separation) for quality control. One recent tooth sample (third molar) was used in interference studies. Archaeological tooth samples were provided by the Museum of Natural History, Vienna. Detailed information on approximate age and context of these archaeological samples can be found elsewhere [35]. Samples were sonicated for approximately 5 minutes in 1 % nitric acid followed by a rinsing step with reagent grade type I water and final sonication in 2-propanol (p.a., Merck). The samples were dried at room temperature. For solution-based MC ICP-MS, entire tooth fragments or a few mg of tooth dentine and enamel, sampled using a dental drill, were digested in a mixture of H_2O_2 and HNO_3 using hot plate (IKA, Staufen, Germany) assisted acid digestion. Perfluoroalkoxy (PFA) screw cap vials (Savillex, Minnetonka, USA) were used

for digestion. Subsequently the digests were Sr/matrix separated using a Sr specific resin (ElChrom Industries, Inc., Darien, IL, USA) according to standard procedures [36] [37].

2.2.2 Carbonate samples

Solid $CaCO_3$ standards were prepared as follows: 0.14 g of a solution of NIST SRM 987 in HNO_3 (1 % *w/w*) with a strontium concentration of 5365 ng g^{-1} were mixed with 0.5 g $CaCO_3$ powder (p.a., precipitated, Merck, Darmstadt, Germany). This slurry was dried in a drying chamber (WTB-Binder, Tuttlingen, Germany) at 100°C to constant weight and the $CaCO_3$ powder was subsequently pressed into a pellet without using an additional binder. The $^{87}Sr/^{86}Sr$ ratio of the solid $CaCO_3$ standard was determined by LA-MC ICP-MS as well as by liquid based MC ICP-MS (after Sr/matrix separation) for quality control [38].

Fish otoliths originating from Austrian freshwater bodies or hatcheries were used as natural biogenic calcium carbonate samples. Details on the origin of the samples as well as on the exact protocol of fish capture and otolith pre-preparation is described elsewhere [39].

Nine marble samples of non-disclosed origin, representing a selected, geological $CaCO_3$ matrix, were investigated for their elemental and Sr isotopic composition. Marble samples were digested using a reagent mixture of 1 mL H_2O_2 and 2 mL double-subboiled HNO_3 following a similar hot-plate assisted digestion procedure as applied for tooth samples. One marble sample (A1) was chosen for recording interference spectra by LA-ICP-SFMS due to its low Rb content.

2.3 Instrumentation and performed experiments

2.3.1 (LA)-ICP-MS for elemental analyses

In case of tooth samples and standard reference materials, elemental ratios were measured using inductively coupled plasma - quadrupole mass spectrometry (ICP-QMS), either by solution-based analysis (in case of sample digests) or by coupling an 'LSX 200' laser ablation system from CETAC Technologies (Omaha, USA) (in case of solid samples) to a PerkinElmer ELAN DRC-e ICP-MS (Perkin Elmer, Ontario, Canada). Typical instrumental parameters are listed in Table 3. Ablation was performed at a repetition rate of 10 Hz and the first 10 seconds of each ablation profile were rejected from data evaluation. Raw signal intensities were *on peak* baseline corrected by subtracting a corresponding gas blank. Single spot analysis was done in replicates of 5-6 for each sample.

2.3.2 LA-ICP-SFMS for interference studies

In order to identify potential interferences and their relative *m*/*z* positions to the isotopes of Kr, Sr and Rb, the following experiment was performed: Transects of two human enamel and one dentine sample, one marble sample, in-house pelletized NIST SRM 1400, NIST SRM 1486 and (Sr containing) $CaCO_3$ as well as one fish otolith were measured at *m*/*z* 82, 83, 84, 85, 86, 87 and 88 during line-scan ablation for approximately one hour time span per sample in medium mass resolution ($m/\Delta m \approx$ 4000; 10 % valley definition) on an 'Element 2' (Thermo Fisher Scientific, Bremen, Germany). Recorded data was integrated over the measurement time. A 'New Wave UP-213' LA system (New Wave Research Inc, Fremont, CA, USA) was coupled to the ICP-SFMS instrument at the Institute of Isotopes of the Hungarian Academy of Sciences in Budapest, Hungary. Typical instrumental parameters are summarized in Table 3.

2.3.3 Solution-based MC ICP-MS

A 'Nu plasma HR' MC ICP-MS instrument (Nu Instruments Ltd, Wrexham, UK) was used for isotopic analyses. Instrumental parameters for routine analysis of digested apatite or carbonate samples as well as for measurements involving standard reference materials are summarized in Table 3. In addition to Sr, isotopic analysis of Rb and Zr standard reference materials and mixtures of the same were performed for investigation of instrumental isotopic fractionation. The instrument was tuned daily for maximum sensitivity and stability. Quad lens settings were optimized for peak shape and alignment for different axial masses set. The detector arrangement is described in detail elsewhere [40] [41]. A 'DSN 100' desolvation nebulisation membrane (Nu Instruments Ltd., Wrexham, UK) was employed for all solution measurements. Blank correction of solution-based MC ICP-MS analysis was performed *on peak* using the *measure zero* method implemented in the Nu Plasma instrument software.

2.3.4 LA-MC ICP-MS for isotopic analyses

An 'LSX 200' LA system (CETAC Technologies, Omaha, USA) and a NWR-193 (ESI - New Wave Research, Fremont CA) were used for sample ablation under Ar and/or He atmosphere. Instrumental parameters are summarized in Table 3.

Recorded raw intensities at *m*/*z* 82, 83, 84, 85, 86, 87 and 88 were *on peak* baseline corrected with a corresponding gas blank measured for 60 seconds before ablation. Gas blanks were re-recorded after change of the ablation target, with a maximum of 6 subsequent ablation events for one target.

Table 3
Operating parameters of the ICP-MS instrumentation and sample introduction systems

MC ICP-MS (Nu Plasma HR)	
Axial mass MC ICP-MS /*m/z*	84, 86, 87, 88
Masses monitored /*m/z*	82, 83, 84, 85, 86, 87, 88
Mass resolution / *(m/z)/(Δm/z)*	~300
Cones	Ni
Detectors	Faraday cups
Data acquisition mode for LA	TRA (time resolved analysis)
Dwell time /s	2
RF power /W	1300
Plasma gas flow /L min^{-1}	13
Auxiliary gas flow /L min^{-1}	0.9-1.2
Data acquisition parameters (solution mode analysis)	
Integration time for solution-mode /s	10
Instrumental sensitivity /V ppm^{-1}	200-400
Number of blocks	6
Measurements per block	10
ICP-SFMS Parameters (ThermoFisher Element 2)	
Cones	Ni
Oxide level /%	~0.5-0.6
Ba^{2+}/Ba^{+}	2 %
Mass resolution /*(m/z)/(Δm/z)*	~300 (LR)/~4000 (MR)
Detector	Secondary electron multiplier
Mass window	800
Scan type	E-scan
Sample time /ms	0.01
Samples per peak	20
Runs x passes	1 x 300
Total measurement time /min	~60
RF power /W	1290
Auxiliary gas flow /L min^{-1}	0.99
ICP-QMS (PerkinElmer Elan DRC-e)	
Sample gas flow rate /L min^{-1}	1.8
RF power	1300
Cones	Ni
Detector	Secondary electron multiplier
Auxiliary gas flow /L min^{-1}	0.98-1.02
Cool gas flow /L min^{-1}	13.7
Analysed isotopes	^{31}P, ^{42}Ca, ^{43}Ca, ^{44}Ca, ^{48}Ca, ^{83}Kr, ^{85}Rb, ^{86}Sr, ^{87}Sr, ^{88}Sr,
LA Parameters (Cetac LSX 200)	
Ablation mode	static point ablation
Laser wave length / nm	266
Ablation gas	Ar
LA-gas flow /L min^{-1}	~1.6
Repetition rate /Hz	10-20
Ablation duration /sec	60
Spot size /µm	100-300
Laser energy per pulse / mJ / energy level	3 / 20 (maximum)
LA Parameters (New Wave UP-213, NWR-193)	
Ablation mode	dynamic line scan
Scan speed / µm s^{-1}	2-5
Depth/pass / µm	2-5
Laser wave length / nm	213/193
Ablation gas	Ar/He
LA-gas flow /L min^{-1}	0.9-1.9
Repetition rate /Hz	10-20
Spot size /µm	50-95
DSN parameters (DSN-100)	
Nebuliser	PFA µ-flow
Nebuliser back pressure /psi	~30
Hot gas flow /L min^{-1}	~0,3
Membrane gas flow /L min^{-1}	~2.8
Spray chamber temperature /°C	~115
Membrane temperature /°C	~120

2.3.5 Common practice correction for instrumental isotopic fractionation of Sr and Rb interference correction

Recently, the term ‘‘instrumental isotopic fractionation’’ (IIF) was recommended to describe the sum of the effects in a mass spectrometer causing a shift of the measured isotope ratio from the true isotope ratio in a sample and will be used throughout the text. IIF is also known as (instrumental) mass bias or (instrumental) mass fractionation in literature [12].

In case of Sr isotope ratios, the instrumental isotopic fractionation of the $^{87}Sr/^{86}Sr$ isotope ratios is commonly calculated using the fractionation factor of the internal $^{88}Sr/^{86}Sr$ isotope ratio in the sample and by applying the Russell’s law for instrumental isotopic fractionation correction (see Equation 1) [42] [43] [44] [12].

$$R_{corr}^{i/j} = R_{meas}^{i/j} \cdot \left(\frac{m_i}{m_j}\right)^f \text{ (Equ. 1)}$$

where R_{meas} and R_{corr} correspond to the measured and true isotope ratios, respectively, m_i and m_j are the nuclide masses of the isotopes of interest, and f is the factor to correct for instrumental isotopic fractionation (also termed ‘‘mass bias factor’’ or ‘‘fractionation factor’’).

However, since it was shown that the $^{88}Sr/^{86}Sr$ isotope ratio shows significant natural fractionation, the application of this calibration strategy was investigated in detail.

External instrumental isotopic fractionation correction was performed in a sample standard bracketing procedure by measuring solutions of certified reference material NIST SRM 987 (certified for its Sr isotopic composition) throughout the measurement sequence.

Rb correction was performed via ‚peak stripping’ and assuming the same instrumental isotopic fractionation for Sr and Rb ($f_{Sr} = f_{Rb}$). This included both instrumental isotopic fractionation correction strategies, whereby f_{Sr} was experimentally determined using solutions of NIST SRM 987. Rubidium correction was performed by deducing the ^{87}Rb contribution at m/z 87 calculated via the recorded blank corrected signal of ^{85}Rb at m/z 85 using a $^{87}Rb/^{85}Rb$ ratio of 2.593 ± 0.002 commonly recommended by the IUPAC [45]. This approach for Rb interference correction has been widely applied in the field [43] [15].

3 RESULTS AND DISCUSSION

3.1 Reference values of Sr, Rb and Zr

The issue of finding a variety of reference values for normalization or instrumental isotopic fractionation correction in literature, respectively, has increasingly been discussed in literature. It is also of major concern in Sr isotopic analysis, where the diversity of used and/or published reference values increases constantly. Table 4 shows a selected set of published as well as used normalization values for $^{88}Sr/^{86}Sr$ and $^{87}Sr/^{86}Sr$, $^{87}Rb/^{85}Rb$ and $^{91}Zr/^{90}Zr$ as well as $^{92}Zr/^{90}Zr$ (Note: Ratios are reproduced as reported in the original publication. Also, the "representative" isotopic composition of the elements of interest is given, as defined by the Commission on Isotopic Abundances and Atomic weights of IUPAC as "the isotopic compositions of chemicals and/or natural materials that may be encountered in the laboratory"[46]).

To give an example, raw data of one single measurement of a solution of NIST SRM 987 was evaluated using different normalization values of the $^{88}Sr/^{86}Sr$ isotope ratio for internal instrumental isotopic fractionation correction of $^{87}Sr/^{86}Sr$. Deviations up to 0.05 % are observed when using different normalization values. Furthermore, in case Sr isotope ratios are expressed as δ-values (relative to the NIST SRM 987), the use of different reference values (or 0-anchor values for δ-isotope notation) for the standard is questionable since isotope data will be compared on an international level.

Additionally, the effect of performing internal instrumental isotopic fractionation correction using the published variation of the $^{88}Sr/^{86}Sr$ ratio is shown. Natural fractionation of the $^{88}Sr/^{86}Sr$ can have significant impact on the $^{87}Sr/^{86}Sr$ ratio if internal instrumental isotopic fractionation correction is performed. Therefore, the use of the $^{88}Sr/^{86}Sr$ ratio for IIF correction has to be strongly reconsidered when analysing natural samples, since deviations are significant with respect to total combined uncertainties. The use of the extremes of reported $^{88}Sr/^{86}Sr$ ratios to the same measurement value of $^{87}Sr/^{86}Sr$ (Note: a value of 0.71034 would be achieved when using the IUPAC representative $^{88}Sr/^{86}Sr$ value) leads to a variation of the corrected $^{87}Sr/^{86}Sr$ from 0.71015 to 0.71089. Further information on the use of different normalization values of $^{88}Sr/^{86}Sr$ and their impact on the $^{87}Sr/^{86}Sr$ can be found in Horsky et al. [47]. In contrast, even though increased uncertainties have to be taken into account (probably deriving from temporal fluctuations in instrumental isotopic fractionation) sample standard bracketing leads to accurate results and thus represents an adequate calibration strategy.

Table 4
Recommended values as given by IUPAC for natural Rb, Sr and Zr isotope abundance ratios as well as values found in literature.

REFERENCE	$^{85}Rb/^{87}Rb$	U_c	$^{87}Rb/^{85}Rb$	U_c	
IUPAC best measurement from a single terrestrial source (Catanzaro, Murphy et al. 1969 [45])	**2.59265**	0.00170	**0.38571**		
IUPAC representative isotopic composition	**2.593**	0.002			
NIST SRM 984 ($RbCl_2$) (certified values)	*2.593*	*0.002*			
(Fietzke, Liebetrau et al. 2008 [48])	2.59300		0.385654		
(Halicz, Segal et al. 2008 [49])	2.5907		0.3860		
(Ohno and Hirata 2007 [40])	2.5931				
(Waight, Baker et al. 2002 [50])			0.38540	0.00019	
(Krabbenhöft, Fietzke et al. 2009 [51])			0.386		
REFERENCE	$^{88}Sr/^{86}Sr$	U_c	$^{86}Sr/^{88}Sr$	$^{87}Sr/^{86}Sr$	U_c
IUPAC best measurement of a single terrestrial source (Moore, Murphy et al. 1982 [52])	**8.37861**	0.00325	**0.11935**	**0.71034**	0.000261
IUPAC representative isotopic composition	**8.37521**			**0.71034**	
NIST SRM 987 ($SrCO_3$) (certified values)	***8.37861***	*0.00325*		***0.71034***	*0.00026*
(Nier 1938 [53])	8.3752		0.1194		
(Liu, You et al. 2012 [54])	8.375209			0.710245	
(Krabbenhöft, Fietzke et al. 2009 [51])	8.375209			0.71024	
(Revel-Rolland, De Deckker et al. 2006 [55])				0.71025	
(Balcaen, De Schrijver et al. 2005 [56])				0.71026	
(Faure and Mensing 2005 [57])				0.710245	
(Fietzke, Liebetrau et al. 2008 [48])			0.1194	0.710248	
(Halicz, Segal et al. 2008 [49])			0.1194		
(Ohno and Hirata 2007 [40])			0.1194	0.71024	
(Yang, Peter et al. 2008 [58])	8.37861		0.1194		
(Knudson, Williams et al. 2010 [14])	8.3752		0.1194		
REFERENCE	$^{91}Zr/^{90}Zr$	U_c	$^{90}Zr/^{91}Zr$	U_c	$^{92}Zr/^{90}Zr$
IUPAC best measurement from a single terrestrial source (Nomura, Kogure et al. 1983 [59])	**0.21814**	0.00022			
IUPAC representative isotopic composition	**0.2184**				
(Ohno, Komiya et al. 2008 [60])	0.2181				
(Hirata and Yamaguchi 1999 [61])			4.5842		
(Waight, Baker et al. 2002 [50])			4.5882		
(Sahoo and Masuda 1997 [62])			4.5874	0.0074	
(Nebel, Mezger et al. 2005 [63]) from (Münker, Weyer et al. 2001 [64])	0.21795				
(Yang, Peter et al. 2008 [58])			4.5745		0.33339

3.2 Observations on instrumental isotopic fractionation

Differences in the instrumental isotopic fractionation of Sr, Rb and Zr isotope pairs were observed, when the instrumental isotopic fractionation factor was determined using Russell's law for instrumental isotopic fractionation correction (Fig. 1). Woodhead et al.[65] and Baxter et al.[66] have further refined the Russell approach, with approaches that are especially applicable to solution-based analysis. In this paper, the original approach by Russell was applied. Reference values for NIST SRM 987 and NIST SRM 984 were used according to the certificates of analysis (see Table 4). Zr was measured since it has been shown in literature to serve as promising alternative for instrumental isotopic fractionation correction of Sr isotope ratios [15]. Reference values for Zr were taken from Nomura, Kogure et al. (1983)[59].

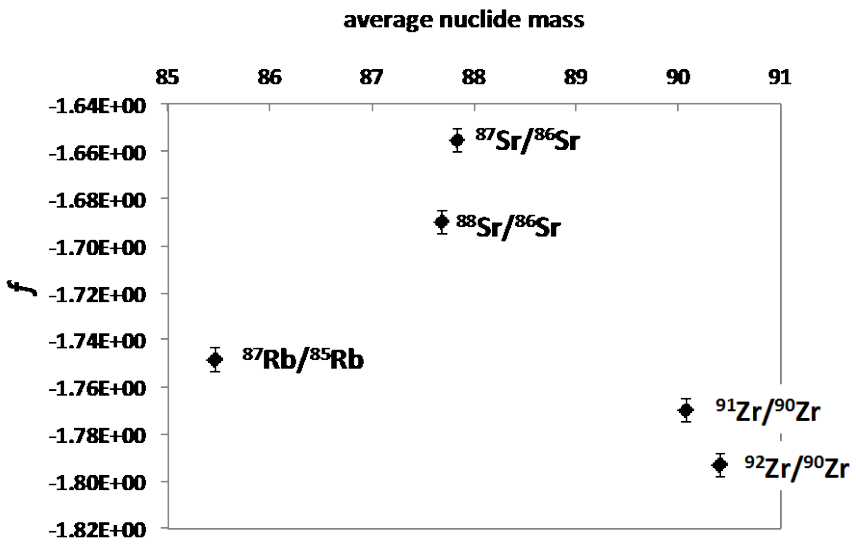

Fig. 1. Instrumental isotopic fractionation factors *f* calculated using the Russell's law for correction of $^{87}Rb/^{85}Rb$, $^{87}Sr/^{86}Sr$, $^{88}Sr/^{86}Sr$, $^{91}Zr/^{90}Zr$ and $^{92}Zr/^{90}Zr$ plotted versus average nuclide mass.

The results for $^{87}Sr/^{86}Sr$ after internal instrumental isotopic fractionation correction of analysing solutions of NIST SRM 987 with increasing Rb concentrations are shown in Fig. 2. $^{87}Sr/^{86}Sr$ ratios were calculated by internal instrumental isotopic fractionation correction using the certified $^{88}Sr/^{86}Sr$ ratio of 8.37861 of the NIST SRM 987 for instrumental isotopic fractionation correction of both Sr and Rb. The dashed lines represent the certified range of the reference material NIST SRM 987. Increasing concentrations of Rb in the sample lead to a systematic increase of the final $^{87}Sr/^{86}Sr$ ratio. Therefore, the conventional approach for Rb correction taking into account the same IIF was once more determined to be inappropriate. This approach leads to inaccurate results for samples with mass fraction ratios of Rb:Sr > 1:50. This has to be considered especially in case of LA analyses, where a separation of Sr from the matrix cannot be accomplished prior to analysis and in cases that significant amounts of Rb are expected. As a consequence, in case samples with increased Rb levels are measured, method validation including experiments of e.g. measuring solutions of Sr with comparable levels of Rb have to be performed in order to investigate the effect of Rb on the $^{87}Sr/^{86}Sr$ ratio or investigating the instrumental isotopic fractionation factor for Rb separately [65, 66]. However, as Ca-rich matrices with low Rb content were investigated in this study, the impact of Rb in the samples was not significant.

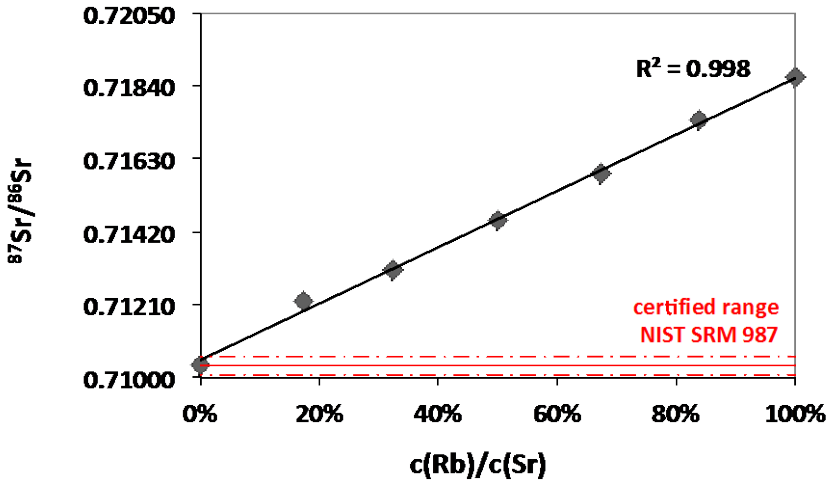

Fig. 2. $^{87}Sr/^{86}Sr$ isotope ratios of solutions of NIST SRM 987 (Sr) with increasing mass fractions of NIST SRM 984 (Rb); data reduction followed common practice corrections (see text).

3.3 Comparison of solution-nebulization-based MC ICP-MS and LA-MC ICP-MS

$^{87}Sr/^{86}Sr$ isotope ratios of all samples and standard reference materials investigated were compared between solution-based MC ICP-MS (after Sr/matrix separation) and LA-MC ICP-MS. The $^{87}Sr/^{86}Sr$ ratios of the analysed carbonates (marble samples, otolith samples and in-house prepared $CaCO_3$ pellets) are significantly decreased in case of LA results, whereas hydroxyl apatite samples (prehistoric tooth samples, certified reference materials of bone matrices (NIST SRM 1400; NIST SRM 1486) and in-house prepared hydroxyapatite pellets) show increased $^{87}Sr/^{86}Sr$ ratios for LA-MC ICP-MS compared to solution-based MC ICP-MS (Table 5).

The mean $\Delta_{LA\text{-}liquid}$ $^{87}Sr/^{86}Sr$ values for each sample type (e.g. tooth dentine, tooth enamel, fish otolith) was calculated as average of all analysed samples of this type along with a standard deviation. It is important to note, that Rb levels in all samples were below a total mass fraction ratio of Rb/Sr = 1/50 (see above). Therefore, the impact of Rb correction is insignificant considering the total combined uncertainties entailed.

The mean absolute $\Delta_{LA\text{-}liquid}$ value of historic tooth dentine samples ranges from 0.00040 to 0.00117 and that of historic tooth enamel samples from 0.00030 to 0.01107. The enamel of the recent tooth sample has a comparable deviation of 0.01133 whereas the recent dentine sample shows an insignificant deviation (overlap within the measurement uncertainties) of -0.00005 due to the significantly higher Sr content as compared to the other dentine samples. The mean $\Delta_{LA\text{-}liquid}$ value for marble samples ranges from -0.00453 to -0.00104. The investigated otolith samples show $\Delta_{LA\text{-}liquid}$ values from -0.00036 to -0.00067 . Based on these results and recent literature in the field (see table 2), it is evident that a number of interferences on the masses of interest (i.e. 85, 86, 87 and 88) have significant impact on the final result since they cause a systematic increase of the $^{87}Sr/^{86}Sr$ ratio in

biological apatite samples and a systematic decrease of $^{87}Sr/^{86}Sr$ in calcium carbonates. Therefore we performed experiments for the study of the elemental composition, especially with respect to Ca, P, Sr and Rb, in tooth and marble samples by solution-based ICP-QMS and LA-ICP-QMS. A correlation of the absolute differences of $^{87}Sr/^{86}Sr$ ratios (obtained by LA and solution-based MC ICP-MS) and $^{42}Ca/^{88}Sr$ and $^{31}P/^{88}Sr$ (obtained by solution-based ICP-QMS and LA-ICP-QMS) was observed (Table 5). This observation underlines even more the presence of molecular interferences. These results make evident that the impact of the Ca and P based interferences on the final $^{87}Sr/^{86}Sr$ ratio depends - as expected - on both the Ca/Sr and the P/Sr ratio in the matrix. Nonetheless, no single correlation can be simply deduced since Ca and P based interferences cause opposite offsets. Since positive offsets are observed, the P based interferences are the dominant source in tooth samples whereas marble samples primarily show Ca based interferences.

Table 5
$^{87}Sr/^{86}Sr$ ratios by (LA)-MC ICP-MS; Sr and Rb concentration and $^{42}Ca/^{88}Sr$; $^{31}P/^{88}Sr$ intensity ratios.

	MC ICP-MS	**LA-MC ICP-MS**			**ICP-QMS**	**ICP-QMS**	**LA-ICP-QMS**	**LA-ICP-QMS**
Tooth samples	**$^{87}Sr/^{86}Sr$ ± 1 *SD***	**$^{87}Sr/^{86}Sr$ ± 1 *SD***	**Δ (LA - liquid)**	**Offset [‰] Δ**	**Sr [µg g^{-}]**	**Rb [µg g^{-1}]**	**$^{42}Ca/^{88}Sr$ [Int/Int]**	**$^{31}P/^{88}Sr$ [Int/Int]**
Archaeological samples								
1 dentine	0.70963±0.00001	0.71020±0.00012	0.00057	0.8	165	0.8	7.87	11.33
		(*n*=5)						
1 enamel	0.70931±0.00001	0.71108±0.00055	0.00177	2.5	125	0.5	7.87	11.33
		(*n*=5)						
92 dentine	0.70999±0.00001	0.71039±0.00141	0.00040	0.6	138	0.2	9.96	13.65
		(*n*=6)						
92 enamel	0.71062±0.00001	0.71305±0.00082	0.00243	3.4	211	0.1	21.56	36.88
		(*n*=5)						
93 dentine	0.70988±0.00001	0.71105±0.00006	0.00117	1.1	170	<0.1	7.88	11.31
		(*n*=5)						
93 enamel	0.71065±0.00001	0.72172±0.00016	0.01107	3.2	70	0.1	21.56	33.09
		(*n*=6)						
94 dentine	0.70941±0.00001	0.70983±0.00009	0.00042	0.6	131	0.5	6.11	9.77
		(*n*=5)						
94 enamel	0.70832±0.00001	0.70862±0.00065	0.00030	0.4	148	0.3	6.99	13.08
Recent tooth sample								
JI-M3 dentine	0.70996±0.00001	0.70991±0.00073	-0.00005	<0.1	350	0.2	-	-
JI-M3 enamel	0.70971±0.00001	0.71109±0.00042	0.01133	2.0	140	0.1	-	-
Reference material		(*n*=5)						
NIST SRM 1486	0.70931±0.00006	0.70964±0.00016	0.00033	0.6	264	-	4.91	8.50
Marble samples								
A1	0.70915 ± 0.00006	0.70781±0.00369	-0.00134	-6.0	40.5	<0.01	12.23	-
		(*n*=6)						
A2	0.70991 ± 0.00006	0.70538±0.00346	-0.00453	-6.4	38.7	<0.01	12.32	-
		(*n*=6)						
A3	0.70962±0.00006	0.70713±0.00062	-0.00249	-3.5	40.3	<0.01	11.30	-
		(*n*=6)						
B1	0.71003±0.00003	0.70899±0.00065	-0.00104	-5.5	43.6	<0.01	10.31	-

		(*n*=6)						
B2	0.71014±0.00006	0.70838±0.00010	-0.00176	-2.5	45.3	<0.01	10.74	-
		(*n*=6)						
B3	0.70946±0.00002	0.70825±0.00049	-0.00121	-1.7	49.3	<0.01	8.76	-
		(*n*=6)						
C1	0.71000±0.00003	0.70612±0.00033	-0.00388	-8.6	37.7	<0.01	11.89	-
		(*n*=6)						
C2	0.71283±0.00005	0.70966±0.00114	-0.00317	-4.4	68.0	<0.01	6.59	-
		(*n*=3)						
C3	0.71106±0.00003	0.70947±0.00046	-0.00159	-2.2	83.2	0.03	5.69	-
		(*n*=6)						
Otolith samples								
otolith 1	0.70785±0.00005	0.70749±0.00045	-0.00036	-0.5				
otolith 2	0.70784±0.00005	0.70717±0.00047	--0.00067	-0.9				
$CaCO_3$ (in-house pelleted)	0.70962±0.00021	0.70944±0.00028	-0.00018	-0.3				-

The offset towards increased $^{87}Sr/^{86}Sr$ ratios and decreased $^{87}Sr/^{86}Sr$ is confirmed and a dependance of the total mass fraction of Sr in the sample is indicated as well as differences between $CaCO_3$ samples and apatite samples. In case of the presence of P in the sample matrix, a shift towards increased $^{87}Sr/^{86}Sr$ isotope ratios can be observed.

3.4 Medium resolution spectra recorded by LA-ICP-SFMS

In order to prove the presence/absence of interferences laser ablation spectra were recorded in medium mass resolution ($(m/z)/(\Delta m/z) \approx 4000$) on a selected set of samples (NIST SRM 1486 pellet, NIST SRM 1400 pellet, tooth dentine T93, tooth enamel T93, tooth enamel T94, otolith 1 and marble A1). Medium mass resolution is able to resolve some of the proposed interferences such as $(^{40}Ar\text{-}^{31}P\text{-}^{16}O)^+$ and $(^{40}Ca\text{-}^{31}P\text{-}^{16}O)^+$ from the Sr and Rb masses, which demand mass resolutions $(m/z)/(\Delta m/z)$ of 3920 and 3883, respectively (Table 1). All Sr masses are potentially interfered by up to three different Ca dimers or Ca-Ar interferences, which cannot be resolved by increasing mass spectrometric resolution as the necessary resolution is above $(m/z)/(\Delta m/z) \approx 10000$, except for $(^{48}Ca^{40}Ca)^+$ where a resolution of 9247 is required. In the following the spectra are given for each m/z recorded:

***m/z* 82 (analyte: $^{82}Kr^{+}$)**

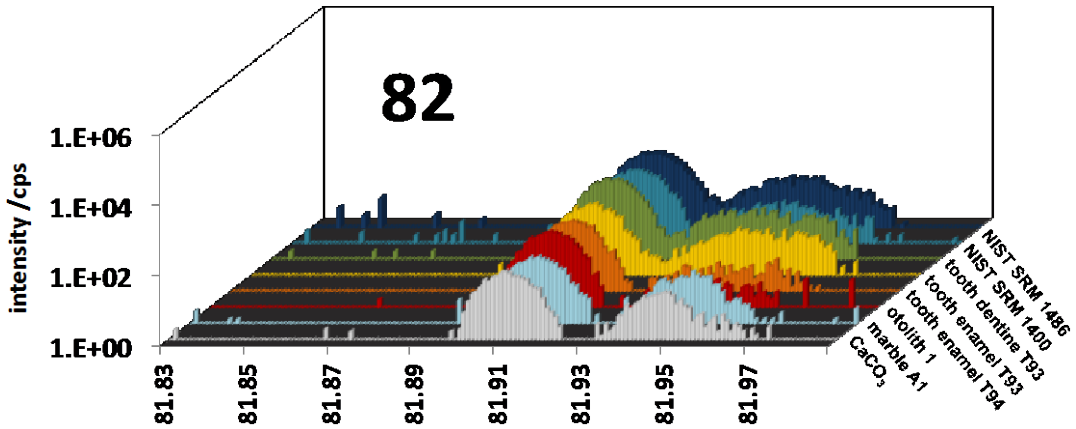

Fig. 3. MR-spectrum *m/z* 82 on selected bioapatite and calcium carbonate samples.

The spectrum obtained at *m/z* 82 (Fig. 3) shows the highest peak at approx. 81.913 and two additional peaks on the high mass side of $^{82}Kr^{+}$ in case of tooth samples as well as the NIST SRM 1486 pellet. In case of the fish otolith, the marble sample and $CaCO_3$ pellet, these additional peaks were less pronounced. According to the mass distances from the $^{82}Kr^{+}$ peak, peak one may represent polyatomic ions such as $(^{40}Ca^{40}Ar^{2}H)^{+}$ or $(^{40}Ar^{40}Ar^{2}H)^{+}$, respectively. The positions of the peak at *m/z* 81.95 agree well with the expected positions of $^{164}Dy^{2+}$ and $^{164}Er^{2+}$.

***m/z* 83 (analyte: $^{83}Kr^{+}$)**

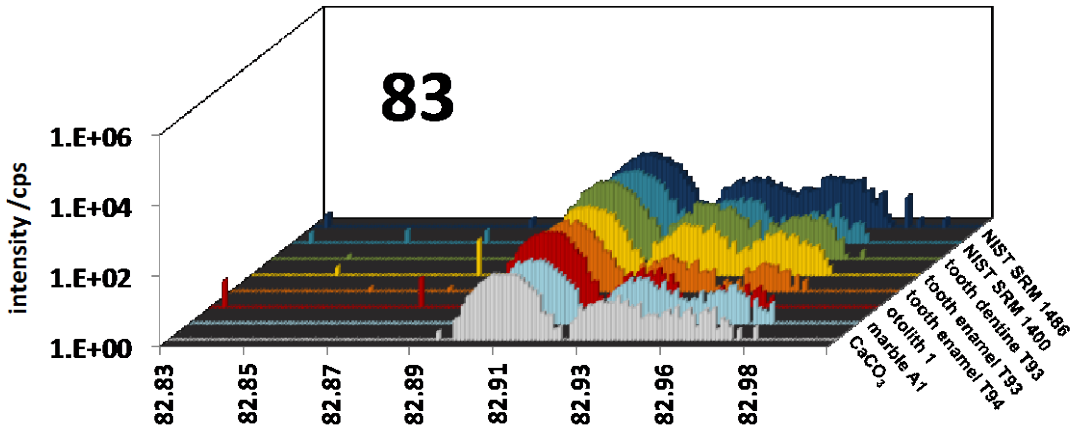

Fig. 4. MR-spectrum *m/z* 83 on selected bioapatite and calcium carbonate samples.

The spectrum obtained at *m/z* 83 (Fig. 4) shows the highest peak at approx. 82.915 and two additional peaks at approx. 82.94 and 82.97, where the peak at a relative mass distance of approx. 0.05 was determined to refer to $^{166}Er^{2+}$ and was found to be present in all sample matrices. Again, signal heights of $^{166}Er^{2+}$ in tooth samples, reference materials and the marble sample exceed that of the investigated fish otolith. The first additional peak appears at a mass distance of approx. 0.025 to

the $^{83}Kr^{+}$ peak (at *m/z* 82.915). $(^{80}Kr^{2}H^{1}H)^{+}$, $(^{40}Ar^{31}P^{12}C)^{+}$, $(^{40}Ca^{31}P^{12}C)^{+}$, $(^{36}Ar^{31}P^{16}O)^{+}$ are a number of possible candidate species for the additional peak and could therefore contribute to the ^{83}Kr signal recorded in low mass resolution.

***m/z* 84 (analytes: $^{84}Kr^{+}$, $^{84}Sr^{+}$)**

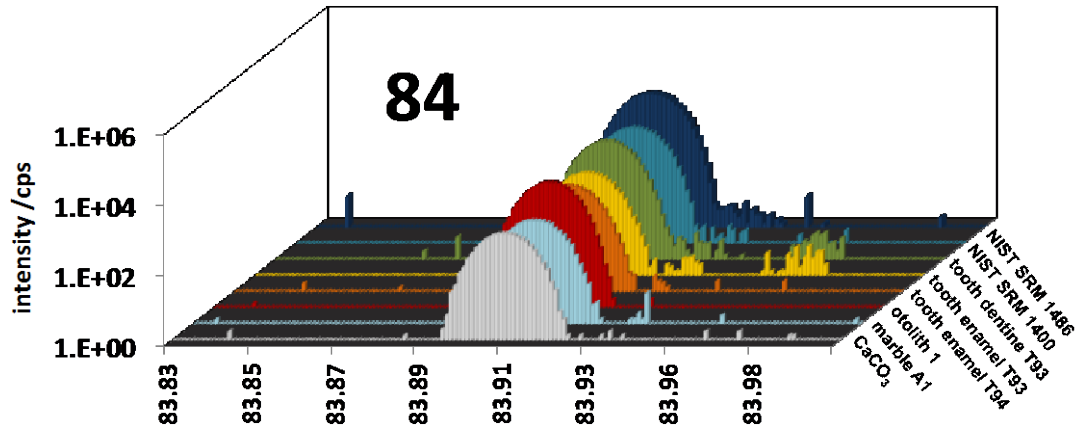

Fig.5. MR-spectrum *m/z* 84 on selected bioapatite and calcium carbonate samples.

The spectrum recorded at *m/z* 84 (Fig. 5) shows the highest peak at approx. 83.913 and therefore reflects the sum of the ^{84}Sr and ^{84}Kr signals. The tooth sample as well as the NIST SRM 1486 pellet show an additional peak at a mass distance to the ^{84}Sr+^{84}Kr peak of approx. 0.025. This peak could represent $(^{42}Ca^{40}Ar^{2}H)^{+}$, $(^{44}Ca^{48}Ar^{2}H)^{+}$, $(^{40}Ar^{31}P^{12}C)^{+}$, $(^{40}Ca^{31}P^{12}C)^{+}$. A second additional peak on the high mass side of the main peak at *m/z* 84 was found for both tooth dentine and enamel of sample T 93 at a mass distance of approx. 0.05, which is likely to be caused by the presence of $^{168}Er^{2+}$ and/or $^{168}Yb^{2+}$, whereas ^{168}Er is significantly more abundant and the two elements do not differ significantly with respect to the first and second ionization potentials. This peak could not be detected for any other sample.

***m/z* 85 (analyte: $^{85}Rb^{+}$)**

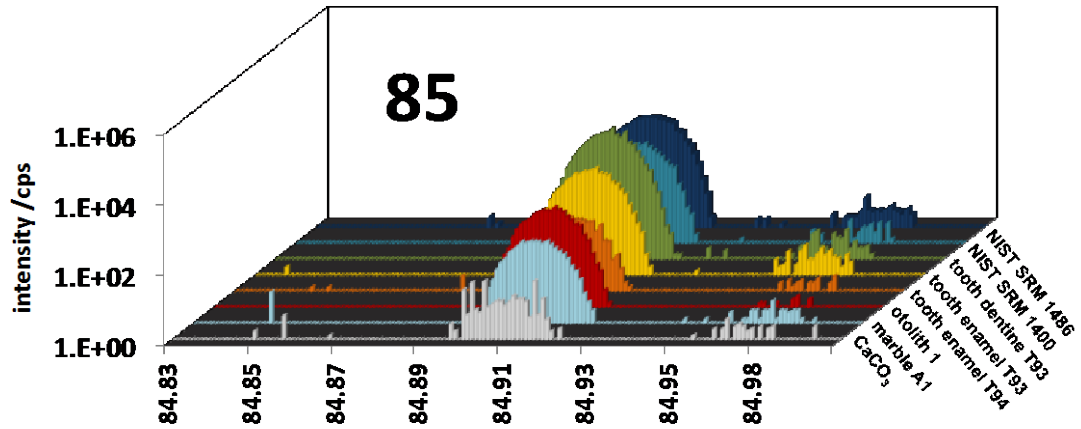

Fig. 6. MR-spectrum *m/z* 85 on selected bioapatite and calcium carbonate samples.

The spectra obtained at *m/z* 85 (Fig. 6) for tooth sample T93 and the NIST SRM 1486 pellet shows the highest peak at approx. 84.91 and one additional peak on the high mass side of the Rb peak at approx. 84.975. The large mass distance of 0.0613 to the Rb peak excludes the presence of interference species composed of Ca, Ar, P, O and H. This is in good agreement with the low abundances of the possible molecular ions composed by these elements at *m/z* 85. A potential Ca dimer cannot be resolved as the required resolution is approx. 15000. With respect to the calculated theoretical mass distance of $^{85}Rb^{+}$ to $^{170}Er^{2+}$ and $^{170}Yb^{2+}$ of approx. 0.0559, the peak could represent of REEs in the samples.

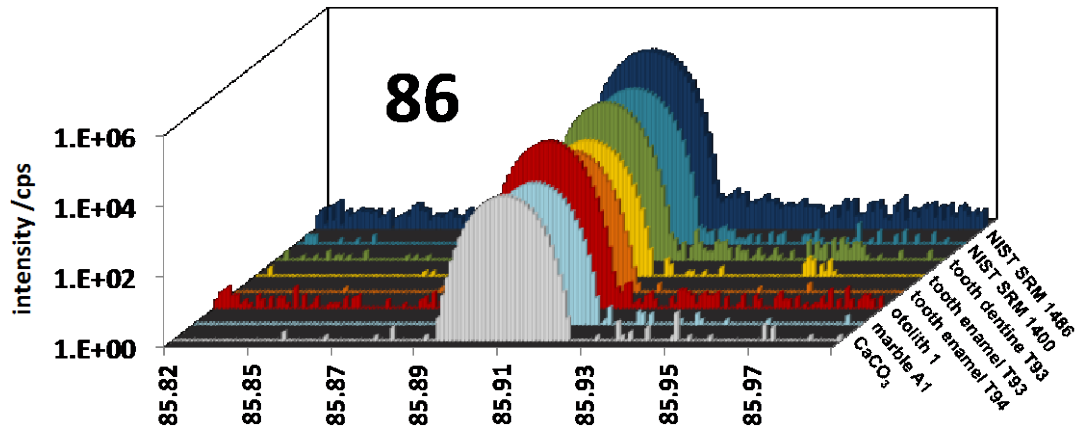

***m/z* 86 (analytes: $^{86}Kr^{+}$, $^{86}Sr^{+}$)**

Fig. 7. MR-spectrum *m/z* 86 on selected bioapatite and calcium carbonate samples

The spectra obtained at *m*/*z* 86 (Fig. 7) shows the highest peak at approx. 85.908 and no significant additional peaks. In case of tooth T93 the presence of $^{172}Yb^{2+}$ has to be considered, however with marginal contribution to the $^{86}Sr^{+}$ peak, since an average of 3–5 cps was counted compared to an average maximum signal of $^{86}Sr^{+}$ of 28000 cps.

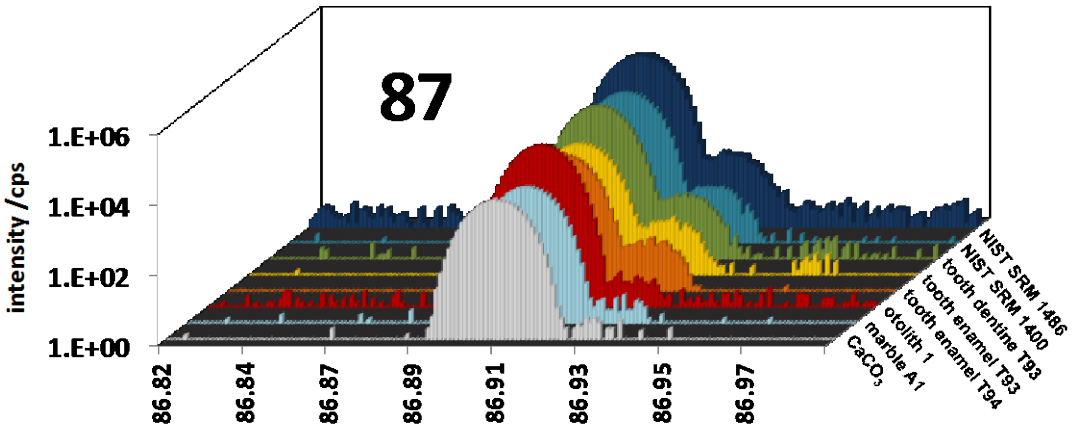

Fig. 8. MR-spectrum *m*/*z* 87 on selected bioapatite and calcium carbonate samples

The spectra obtained at *m*/*z* 87 (Fig. 8) shows the highest peak at approx. 86.908. The interferences found on *m*/*z* 87 reflect the observations of a systematic increase of the $^{87}Sr/^{86}Sr$ isotope ratio in hydroxyl-apatite matrices measured by LA-MC ICP-MS compared to solution analysis after Sr/matrix separation. It is likely that the peak at approx. 86.935 is caused by molecular ions of $(^{40}Ca\text{-}^{31}P\text{-}^{16}O)^{+}$ and $(^{40}Ar\text{-}^{31}P\text{-}^{16}O)^{+}$. The mass distance of the sole additional peak found correlates well with the calculated mass distance and contributes up to 0.2 - 0.8 % of the Sr intensity at *m*/*z* 87 for apatite samples. This effect is found to be similarly pronounced in dentine and enamel of sample T93 as well as NIST SRM 1400 and 1486 pellets. Even though the peak at this mass distance was also found for the $CaCO_3$ pellet, the fish otolith and the marble sample, its contribution to the final ^{87}Sr signal is comparably low with relative heights of 0.01-0.09 % of the $^{87}Sr^{+}$ signal. For the tooth sample one small additional peak was found at a mass distance of approx. 0.06, which indicates the presence of $^{174}Yb^{2+}$ and $^{174}Hf^{2+}$, with its contribution amounting to less than 0.02 % of the $^{87}Sr^{+}$ signal.

***m/z* 88 (analyte: $^{88}Sr^{+}$)**

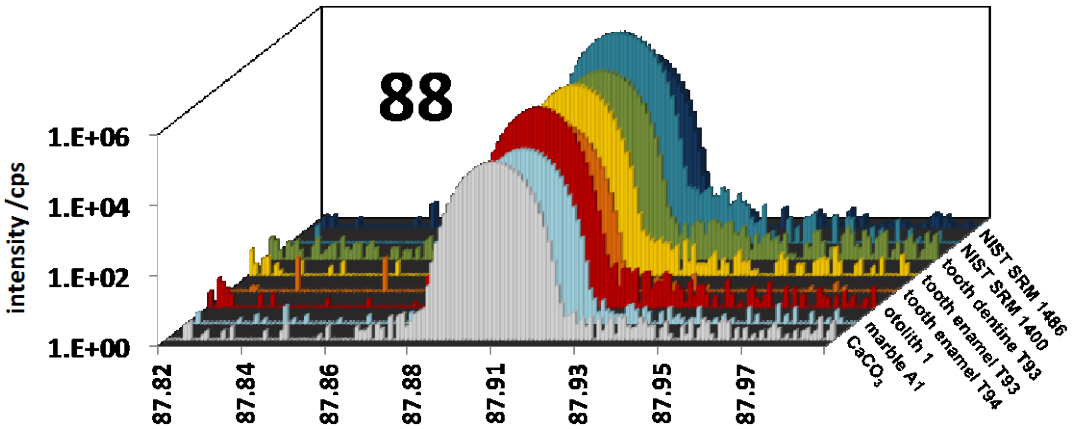

Fig. 9. MR-spectrum *m/z* 88 on selected bioapatite and calcium carbonate samples

The spectra obtained at *m/z* 88 (Fig. 9) shows the highest peak at approx. 87.904 and suggest the presence of $(^{40}Ca\text{-}^{31}P\text{-}^{17}O)^{+}$ and $(^{40}Ar\text{-}^{31}P\text{-}^{17}O)^{+}$. The presence of REEs ($^{176}Yb^{2+}$, $^{176}Hf^{2+}$, $^{176}Lu^{2+}$) could not be seen in the investigated samples, which could be explained by the lower abundances of the respective isotopes compared to the lower masses investigated, where doubly charged REE isotopes were detected.

The observed spectra clearly show the presence of additional components at all observed masses other than the analyte isotopes of interest. Having a closer look at *m/z* 87, where the molecular species $(^{40}Ca\text{-}^{31}P\text{-}^{16}O)^{+}$ and $(^{40}Ar\text{-}^{31}P\text{-}^{16}O)^{+}$ are expected, a correlation of the additional peak at the high mass side and the Sr mass fraction in a sample can be found (Fig. 10). Therefore, we can deduce that the intensity of the interfering peak remains constant within comparable matrices (i.e. hydroxyl apatite matrices). This is shown on the example of NIST SRM 1400, NIST SRM 1486 and tooth dentine and enamel (T93), where the signal intensity of the additional peak was set in relation to the peak of $^{87}Sr^{+}$ and plotted versus the total mass fraction of Sr in the samples. The observation underlines the assumption of the significance of P-based interferences to strongly depend on the total Sr mass fraction and thus leads to a significant shift in the $^{87}Sr/^{86}Sr$ ratios at low Sr concentrations. From a Sr concentration of approx. 200 µg g^{-1}, the interfering peak can be estimated as insignificant with respect to the measurement uncertainties of LA-MC ICP-MS (see Table 6). Nonetheless, a correction factor can be calculated from the relationship shown in Fig. 10 and provides a potential correction strategy.

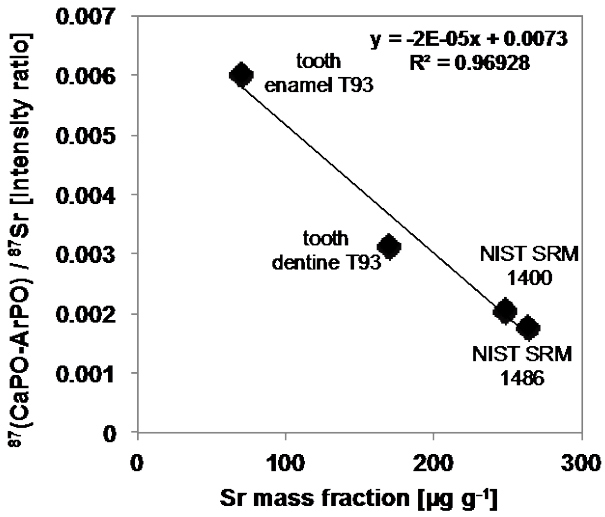

Fig. 10. Sr mass fraction plotted versus ^{87}(CaPO-ArPO)/^{87}Sr intensity ratio

3.5 LA-MC ICP-MS measurements of selected samples to monitor presence of Ca dimers and Ca argides

The presence and significance of Ca-based interferences during LA analysis has been discussed controversially in literature. In order to verify whether Ca dimers and argides are present in the analytical setup used during LA-MC ICP-MS analysis, data obtained at *m*/*z* 82 and 83 during line scan analysis (duration 450 s) of a homogeneous fish otolith samples were evaluated in detail, where we expect only Ca dimers as interferences in addition to the signals of the Kr isotopes. In case of absence of interferences, we would expect a ratio of 1.009 for natural ^{82}Kr/^{83}Kr. In case of the presence of Ca dimers, we would expect a shift to a ratio of 4.7 according to the natural abundance of Ca isotopes in the dimers and Ar interferences (^{82}(^{40}Ca^{42}Ca+^{42}Ca^{40}Ar)$^{+}$ / ^{83}(^{40}Ca^{43}Ca+^{43}Ca^{40}Ar)$^{+}$) (see Table 1). The latter assumption was verified (see Fig. 11). In contrast to the blank recorded prior to ablation, where the natural ^{82}Kr/^{83}Kr ratio of 1.009 was observed from the background gas, an intensity ratio at *m*/*z* 82 and 83 of 4.7 (*I-82*/*I-83*) was observed during sample analyses, correspond to the expected value of Ca and Ar interferences.

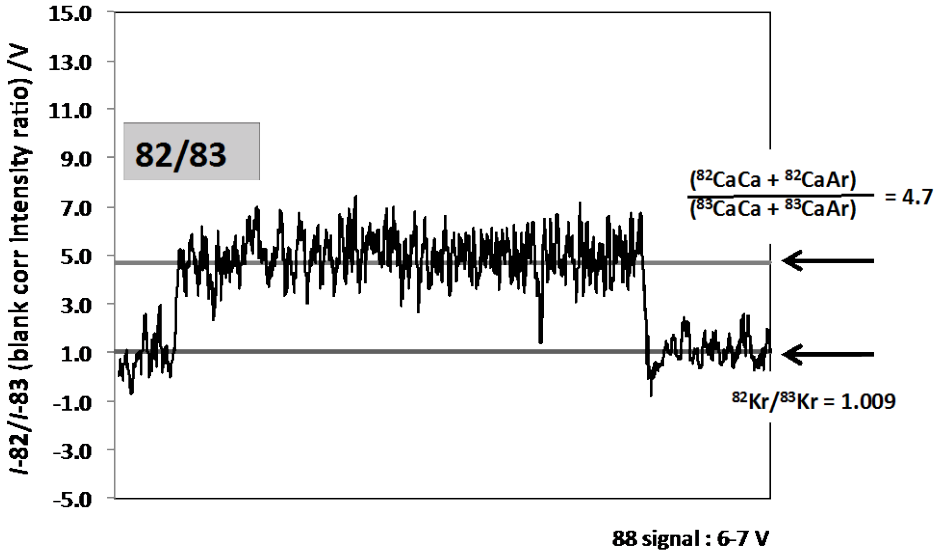

Fig. 11. LA-MC ICP-MS time resolved signal *I-82*/*I-83* (V) during analysis of an otolith sample for monitoring the presence of Ca-based interferences.

3.6 Correction for Ca/P-based interferences – Mathematical approximations

Based on the regression obtained in Fig. 11 as well as the signal intensities obtained during MC ICP-MS analysis at *m*/*z* 82 and 83 for Ca dimers and Ca argides, the contribution of Ca/P-based interferences to the signal intensities on the Sr masses were estimated and a $^{87}Sr/^{86}Sr$ correction for laser ablation data was performed as following:

1. Blank correction on-peak for all measured isotopes (*m*/*z* 82, 83, 84, 85, 86, 87, 88)
2. CaCa/CaAr correction calculated from blank corrected signals at *m*/*z* = 82; 83 via natural abundances of Ca and Ar. Therefore, the signal contributions of CaCa/CaAr interferences on *m*/*z* 84, 85, 86, 87 and 88 were calculated based on the obtained signal at *m*/*z* = 82 using the abundances listed in Table 1. No IIF correction was performed.

3. CaPO/ArPO correction via 87-interference correction factor calculated based on Sr concentration and interference/signal ratio. The correlation obtained in Fig. 10 allows (based on the knowledge of the Sr mass fraction in the sample and the Sr/P and Sr/Ca elemental composition) a calculation of the $(^{40}Ca\text{-}^{31}P\text{-}^{16}O)^+$ and $(^{40}Ar\text{-}^{31}P\text{-}^{16}O)^+$ - intensity relative to the intensity obtained for ^{87}Sr. A correction can be performed and the signal intensity of the *m*/*z* 87 beam leads to a corrected beam intensity that subsequently follows 'conventional' corrections (i.e. Rb interference correction and IIF correction).
4. Rb correction via peak stripping using the Russell law and assuming *f*(Sr) = *f*(Rb) since the Rb/Sr mass fraction ratio < 1:50

5. Instrumental isotopic fractionation correction via external correction following standard sample bracketing using the correction factor obtained for Sr by measuring solutions of NIST SRM 987.

The data corrections were performed on a selected set of samples (JI-M3 tooth dentine, JI-M3 tooth enamel and otolith 1 and otolith 2) for which additional medium resolution spectra were obtained and which were not used to calculate the regression (Fig. 10). The results of the correction are shown in Fig. 12. Correction of calcium dimers/argides as well as P-based interferences (in case of bioapatite samples) yields agreement of $^{87}Sr/^{86}Sr$ ratios from laser ablation compared to solution-based measurements within uncertainties. Calcium dimer/argide correction solely does not lead to accurate results for tooth enamel as can be seen from Fig. 12. An addition correction for P-based interferences is necessary.

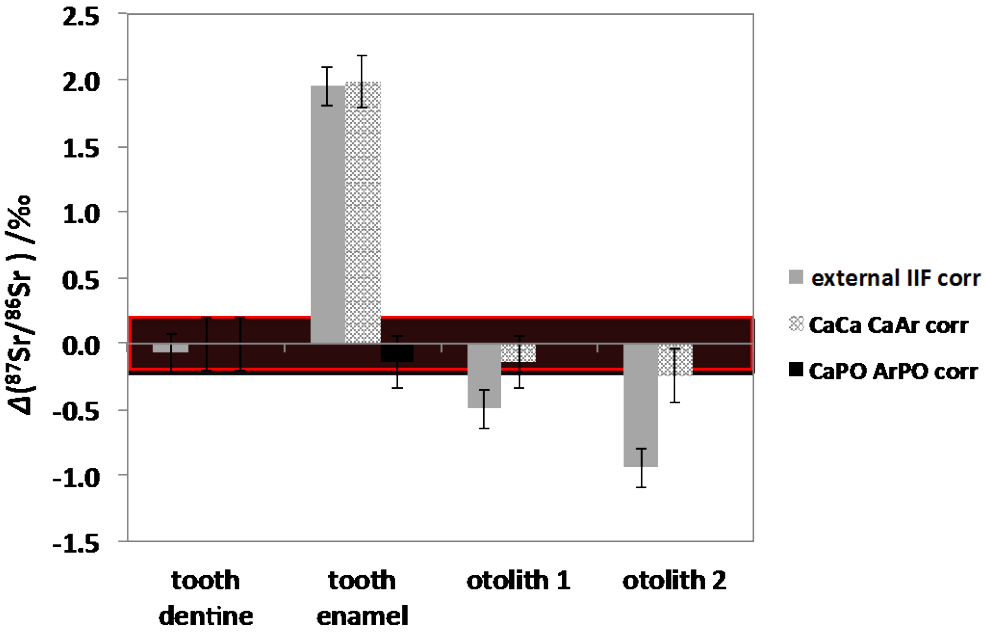

Fig. 12. $\Delta^{87}Sr/^{86}Sr$ ratios (solution vs. laser) results after stepwise correction for interferences; the red bar indicates combined uncertainties of solution-based analysis after sample digestion and Sr/matrix separation (Samples: JI-M3 dentine, JI-M3 enamel, otolith 1, otolith 2).

3.7 Total combined uncertainty calculation

Total combined uncertainties were calculated according to the *Guide to the Expression of Uncertainty in Measurement* (JCGM100:2008 2012) guidelines [67] and using the Kragten approach of uncertainty calculation [68]. Uncertainty considerations are based on Horsky et al. [47], where details about uncertainty calculations can be found. The calculation of combined uncertainties for solution-based analysis of the $^{87}Sr/^{86}Sr$ ratio yields an expanded uncertainty of 0.024 % ($U_{c,rel}$, k=2) when

including the propagation of the uncertainty given for the IUPAC reference values [69], which accounts for 99 % of the expanded total combined uncertainty. Thus, calculations were further done excluding the reference value as information on the uncertainties of the method parameter was of interest. Blank, Rb correction and measurement precision were considered and propagated accordingly. [47]The calculation of combined uncertainties excluding the propagation of the uncertainties given for the IUPAC $^{88}Sr/^{86}Sr$ reference value would yield a value of 0.0022 % ($U_{c,rel}$, k=2), whereby the main contributors are listed in Table 6. This indicates clearly, that the calculation of absolute values yields a larger uncertainty as compared to values, which are calibrated relatively to a reference standard (NIST SRM 987). Thus, delta values seem to be much more relevant in tracer studies when only relative differences of the isotopic composition have to be considered and thus the uncertainty of the absolute ratios of the reference standard has not to be taken into account (note: only the heterogeneity of the reference standard would contribute to the uncertainty).

The calculation of combined uncertainties for laser ablation analysis of the absolute $^{87}Sr/^{86}Sr$ ratio yields an expanded uncertainty of 0.083 % ($U_{c,rel}$, k=2) for calculations including the propagation of the uncertainty given for the IUPAC $^{88}Sr/^{86}Sr$ reference value [69] used for internal instrumental isotopic fractionation correction. The calculation of combined uncertainties excluding the propagation of the uncertainties given for the IUPAC $^{88}Sr/^{86}Sr$ reference value yields a value of 0.080 % ($U_{c,rel}$, k=2). The main contributors to the uncertainty are listed in Table 6.

Table 6
Single input parameters to the total combined uncertainties U_c (k=2) for solution-based and LA-MC ICP-MS.

Setup	Parameters	Relative contribution /%
Solution-based MC ICP-MS	*U*-blank	12
	U-Rb	1
	U-measurement precision	87
	Total uncertainty $U_{c,rel}$ *(k = 2)*	0.0022 %
LA-MC ICP-MS	*U*-blank	9.5
	U-Rb	90.3
	U- measurement precision	0.2
	Total uncertainty $U_{c,rel}$ *(k = 2)*	0.080 %

4 CONCLUSIONS

This study underlines the complex matter of Sr isotope ratio measurements by means of LA-MC ICP-MS and the challenges entailed. We showed that the approaches presented so far offer promising possibilities to cope with the problems entailed in Sr isotope ratios measurements by LA-MC ICP-MS. The biggest challenges can certainly be assigned to the correction of instrumental isotopic

fractionation and interferences. The presence of interferences is without accepted controversy for the system used in this study. Interferences were shown to be present in all sample matrices investigated and consequently have significant impact to measured Sr isotope ratios by LA-MC ICP-MS. However, the significance of Ca- and P- based interferences strongly depends on the Sr mass fraction in the sample. The contribution of Ca- and P- based interferences can be determined if Ca, P and Sr mass fractions in the samples are known. Thus, Sr isotope ratios obtained by LA-MC ICP-MS in samples such as seawater otoliths might not be significantly biased, as lower amounts of sample matrix are sufficient for isotopic analysis.

Further, we confirmed that the TIMS-based Russell law of instrumental isotopic fractionation correction does not compensate for all instrumental isotopic fractionation processes occurring in a MC ICP-MS instrument. Therefore, its use for MC ICP-MS might have to be reconsidered especially if multiple isotopic systems are taken into account (e.g. in this case Rb as interference, Sr as analyte and Zr as possible system for instrumental isotopic fractionation correction).

We summarize that instrumental isotopic fractionation and interferences in Sr isotope ratio analyses demand clear and well reported strategies comprising the analytical protocol starting from sample preparation over the measurement itself to data handling including all corrections performed, which are (1) blank and Kr correction, (2) correction of instrumental isotopic fractionation, (3) Rb correction, (4) correction for Ca-Ar molecular interferences, and (5) other molecular species stemming from the major matrix elements (Ar-P-O; Ca-P-O). These strategies might differ strongly between different labs, instrumentations used (i.e. MC ICP-MS; LA-systems) and sample type (especially considering different mass fractions of Sr). Sample heterogeneity and variations in formation and stability of such interferences may however differ strongly between natural samples and makes the establishment and applicability of a ‘ready-to-use’ measurement method and data evaluation protocol a delicate matter. However, the corrections applied have to – under consideration of the increasing uncertainties with every additional correction step implemented – meet the individual question’s requirement and have – above all – to be described in detail whenever Sr isotope ratios are reported.
With respect to the continuous increase of expanded uncertainties with each correction step applied, the limitations of the use of LA-MC ICP-MS have to be considered.

ACKNOWLEDGEMENTS

This work was supported by the Austrian Science Fund FWF (START project 267N11, Isomark Project P21404-B17) and the Austrian Academy of Sciences, DOC-fForte fellowship programme. We

acknowledge Maria Teschler-Nicola from the Natural History Museum Vienna, Department of Anthropology and Alexandra Krenn-Leeb from the University of Vienna, Department of Prehistory for providing the analyzed tooth samples, Andreas Zitek for providing fish otoliths samples and fruitful discussions and Josef Strobl and Christopher Weiß for technical support in the lab. Many thanks go to Zsolt Stefánka for making the measurements in his lab facilities at the Institute of Isotopes in Budapest, Hungarian Academy of Science, possible.

REFERENCES

1. Kennedy, B.P., J.D. Blum, C.L. Folt, and K.H. Nislow, *Using natural strontium isotopic signatures as fish markers: Methodology and application.* Can. J. Fish. Aquat. Sci., 2000. **57**(11): p. 2280-2292.
2. Kennedy, B.P., A. Klaue, J.D. Blum, C.L. Folt, and K.H. Nislow, *Reconstructing the lives of fish using Sr isotopes in otoliths.* Can. J. Fish. Aquat. Sci., 2002. **59**(6): p. 925-929.
3. Clarke, A.D., K.H. Telmer, and J. Mark Shrimpton, *Elemental analysis of otoliths, fin rays and scales: A comparison of bony structures to provide population and life-history information for the Arctic grayling (Thymallus arcticus).* Ecol. Freshwat. Fish, 2007. **16**(3): p. 354-361.
4. Montgomery, J., *Passports from the past: Investigating human dispersals using strontium isotope analysis of tooth enamel.* Ann Hum Biol, 2010. **37**(3): p. 325-346.
5. Vroon, P.Z., B. Van Der Wagt, J.M. Koornneef, and G.R. Davies, *Problems in obtaining precise and accurate Sr isotope analysis from geological materials using laser ablation MC-ICPMS.* Anal. Bioanal. Chem., 2008. **390**(2): p. 465-476.
6. Balcaen, L., L. Moens, and F. Vanhaecke, *Determination of isotope ratios of metals (and metalloids) by means of inductively coupled plasma-mass spectrometry for provenancing purposes - A review.* Spectrochimica Acta - Part B Atomic Spectroscopy, 2010. **65**(9-10): p. 769-786.
7. Latkoczy, C., T. Prohaska, G. Stingeder, and M. Teschler-Nicola, *Strontium isotope ratio measurements in prehistoric human bone samples by means of high-resolution inductively coupled plasma mass spectrometry (HR-ICP-MS).* J. Anal. At. Spectrom., 1998. **13**(6): p. 561-566.
8. Latkoczy, C., T. Prohaska, M. Watkins, M. Teschler-Nicola, and G. Stingeder, *Strontium isotope ratio determination in soil and bone samples after on-line matrix separation by coupling ion chromatography (HPIC) to an inductively coupled plasma sector field mass spectrometer (ICP-SFMS).* J. Anal. At. Spectrom., 2001. **16**(8): p. 806-811.
9. Prohaska, T., C. Latkoczy, G. Schultheis, M. Teschler-Nicola, and G. Stingeder, *Investigation of Sr isotope ratios in prehistoric human bones and teeth using laser ablation ICP-MS and ICP-MS after Rb/Sr separation.* J. Anal. At. Spectrom., 2002. **17**(8): p. 887-891.
10. Webb, E., D. Amarasiriwardena, S. Tauch, E.F. Green, J. Jones, and A.H. Goodman, *Inductively coupled plasma-mass (ICP-MS) and atomic emission spectrometry (ICP-AES): Versatile analytical techniques to identify the archived elemental information in human teeth.* Microchem. J., 2005. **81**(2): p. 201-208.
11. Christensen, J.N., A.N. Halliday, D.C. Lee, and C.M. Hall, *In situ Sr isotopic analysis by laser ablation.* Earth. Planet. Sci. Lett., 1995. **136**(1-2): p. 79-85.
12. Irrgeher, J. and T. Prohaska, *CHAPTER 6 Instrumental Isotopic Fractionation*, in *Sector Field Mass Spectrometry for Elemental and Isotopic Analysis*. 2015, The Royal Society of Chemistry. p. 107-120.

13. Fietzke, J. and A. Eisenhauer, *Determination of temperature-dependent stable strontium isotope (δ88Sr/86Sr) fractionation via bracketing standard MC-ICP-MS.* Geochem. Geophys. Geosyst., 2006. **7**(8).
14. Knudson, K.J., H.M. Williams, J.E. Buikstra, P.D. Tomczak, G.W. Gordon, and A.D. Anbar, *Introducing δ88/86Sr analysis in archaeology: A demonstration of the utility of strontium isotope fractionation in paleodietary studies.* J Archaeol Sci, 2010. **37**(9): p. 2352-2364.
15. Irrgeher, J., T. Prohaska, R.E. Sturgeon, Z. Mester, and L. Yang, *Determination of Strontium Isotope Ratios in a Biological Tissue using MC-ICPMS.* Analytical Methods, 2013. **5**(7): p. 1687-1694.
16. Neymark, L.A., W.R. Premo, N.N. Mel'nikov, and P. Emsbo, *Precise determination of δ 88 Sr in rocks, minerals, and waters by double-spike TIMS: a powerful tool in the study of geological, hydrological and biological processes.* J. Anal. At. Spectrom., 2014. **29**(1): p. 65-75.
17. Copeland, S.R., M. Sponheimer, P.J. Le Roux, V. Grimes, J.A. Lee-Thorp, D.J. De Ruiter, and M.P. Richards, *Strontium isotope ratios (87Sr/86Sr) of tooth enamel: A comparison of solution and laser ablation multicollector inductively coupled plasma mass spectrometry methods.* Rapid Commun. Mass Spectrom., 2008. **22**(20): p. 3187-3194.
18. Horstwood, M.S.A., J.A. Evans, and J. Montgomery, *Determination of Sr isotopes in calcium phosphates using laser ablation inductively coupled plasma mass spectrometry and their application to archaeological tooth enamel.* Geochim. Cosmochim. Acta, 2008. **72**(23): p. 5659-5674.
19. Richards, M., K. Harvati, V. Grimes, C. Smith, T. Smith, J.J. Hublin, P. Karkanas, and E. Panagopoulou, *Strontium isotope evidence of Neanderthal mobility at the site of Lakonis, Greece using laser-ablation PIMMS.* J Archaeol Sci, 2008. **35**(5): p. 1251-1256.
20. Nowell, G.M. and M.S.A. Horstwood, *Comments on Richards et al., Journal of Archaeological Science 35, 2008 "Strontium isotope evidence of Neanderthal mobility at the site of Lakonis, Greece using laser-ablation PIMMS".* J Archaeol Sci, 2009. **36**(7): p. 1334-1341.
21. Richards, M., V. Grimes, C. Smith, T. Smith, K. Harvati, J.-J. Hublin, P. Karkanas, and E. Panagopoulou, *Response to Nowell and Horstwood (2009).* J Archaeol Sci, 2009. **36**(7): p. 1657-1658.
22. Copeland, S.R., M. Sponheimer, J.A. Lee-Thorp, P.J. le Roux, D.J. de Ruiter, and M.P. Richards, *Strontium isotope ratios in fossil teeth from South Africa: Assessing laser ablation MC-ICP-MS analysis and the extent of diagenesis.* J Archaeol Sci, 2010. **37**(7): p. 1437-1446.
23. Woodhead, J., S. Swearer, J. Hergt, and R. Maas, *In situ Sr-isotope analysis of carbonates by LA-MC-ICP-MS: Interference corrections, high spatial resolution and an example from otolith studies.* J. Anal. At. Spectrom., 2005. **20**(1): p. 22-27.
24. Yang, Y.-H., F.-Y. Wu, L.-W. Xie, Z.-Y. Chu, and J.-H. Yang, *Re-evaluation of interferences of doubly charged ions of heavy rare earth elements on Sr isotopic analysis using multi-collector inductively coupled plasma mass spectrometry.* Spectrochimica Acta Part B: Atomic Spectroscopy, 2014. **97**: p. 118-123.
25. Müller, W. and R. Anczkiewicz, *Accuracy of laser-ablation (LA)-MC-ICPMS Sr isotope analysis of (bio) apatite–a problem reassessed.* J. Anal. At. Spectrom., 2016. **31**(1): p. 259-269.
26. Bolea-Fernandez, E., L. Balcaen, M. Resano, and F. Vanhaecke, *Tandem ICP-mass spectrometry for Sr isotopic analysis without prior Rb/Sr separation.* J. Anal. At. Spectrom., 2016. **31**(1): p. 303-310.
27. Outridge, P.M., S.R. Chenery, J.A. Babaluk, and J.D. Reist, *Analysis of geological Sr isotope markers in fish otoliths with subannual resolution using laser ablation-multicollector-ICP-mass spectrometry.* Environ. Geol., 2002. **42**(8): p. 891-899.
28. Bizzarro, M., A. Simonetti, R.K. Stevenson, and S. Kurszlaukis, *In situ Sr-87/Sr-86 investigation of igneous apatites and carbonates using laser-ablation MC-ICP-MS.* Geochim. Cosmochim. Acta, 2003. **67**(2): p. 289-302.
29. Jackson, M.G. and S.R. Hart, *Strontium isotopes in melt inclusions from Samoan basalts: Implications for heterogeneity in the Samoan plume.* Earth. Planet. Sci. Lett., 2006. **245**(1-2): p. 260-277.

30. Simonetti, A., M.R. Buzon, and R.A. Creaser, *In-situ elemental and sr isotope investigation of human tooth enamel by laser ablation-(MC)-ICP-MS: Successes and pitfalls.* Archaeometry, 2008. **50**: p. 371-385.
31. Yang, Z., B.J. Fryer, H.P. Longerich, J.E. Gagnon, and I.M. Samson, *785 nm femtosecond laser ablation for improved precision and reduction of interferences in Sr isotope analyses using MC-ICP-MS.* J. Anal. At. Spectrom., 2011. **26**(2): p. 341-351.
32. Wu, F.Y., Y.H. Yang, M.A.W. Marks, Z.C. Liu, Q. Zhou, W.C. Ge, J.S. Yang, Z.F. Zhao, R.H. Mitchell, and G. Markl, *In situ U-Pb, Sr, Nd and Hf isotopic analysis of eudialyte by LA-(MC)-ICP-MS.* Chem. Geol., 2010. **273**(1-2): p. 8-34.
33. Galler, P., A. Limbeck, S.F. Boulyga, G. Stingeder, T. Hirata, and T. Prohaska, *Development of an on-line flow injection Sr/matrix separation method for accurate, high-throughput determination of Sr isotope ratios by multiple collector-inductively coupled plasma-mass spectrometry.* Anal. Chem., 2007. **79**(13): p. 5023-5029.
34. De Muynck, D., G. Huelga-Suarez, L. Van Heghe, P. Degryse, and F. Vanhaecke, *Systematic evaluation of a strontium-specific extraction chromatographic resin for obtaining a purified Sr fraction with quantitative recovery from complex and Ca-rich matrices.* J. Anal. At. Spectrom., 2009. **24**(11): p. 1498-1510.
35. Ehgarner, W., *Die Schädel aus dem frühbronzezeitlichen Gräberfeld von Hainburg, Nieder Österreich..* Mitteilungen der Anthropol. Ges. in Wien 1959. **88/89**: p. 8-90.
36. Swoboda, S., M. Brunner, S.F. Boulyga, P. Galler, M. Horacek, and T. Prohaska, *Identification of Marchfeld asparagus using Sr isotope ratio measurements by MC-ICP-MS.* Anal. Bioanal. Chem., 2008. **390**(2): p. 487-494.
37. Irrgeher, J., M. Teschler-Nicola, K. Leutgeb, C. Weiß, K. Daniela, and P. Thomas, *Migration and Mobility in the Latest Neolithic of the Traisen Valley, Lower Austria − Sr Isotope Analysis.* Conference proceedings - TOPOI Conference on Migrations in Prehistory and Early History, Berlin 2010, 2012.
38. Sturm, M., *Migration studies of fish by measurement of strontium isotope ratios and multi-elemental patterns in otoliths using LA-ICP-MS*, in *Department of Chemistry*. 2008, University of Natural Resources and Life Sciences VIenna: Vienna.
39. Zitek, A., M. Sturm, H. Waidbacher, and T. Prohaska, *Discrimination of wild and hatchery trout by natural chronological patterns of elements and isotopes in otoliths using LA-ICP-MS.* Fish. Manage. Ecol., 2010. **17**(5): p. 435-445.
40. Ohno, T. and T. Hirata, *Simultaneous determination of mass-dependent isotopic Fractionation and radiogenic isotope variation of strontium in geochemical samples by multiple collector-ICP-mass spectrometry.* Anal. Sci., 2007. **23**(11): p. 1275-1280.
41. Brunner, M., R. Katona, Z. Stefanka, and T. Prohaska, *Determination of the geographical origin of processed spice using multielement and isotopic pattern on the example of Szegedi paprika.* Eur. Food Res. Technol., 2010. **231**(4): p. 623-634.
42. Russell, W.A., D.A. Papanastassiou, and T.A. Tombrello, *Ca isotope fractionation on the Earth and other solar system materials.* Geochim. Cosmochim. Acta, 1978. **42**(8): p. 1075-1090.
43. Ehrlich, S., I. Gavrielia, L.B. Dorb, and L. Halicz, *Direct high-precision measurements of the 87Sr/86Sr isotope ratio in natural water, carbonates and related materials by multiple collector inductively coupled plasma mass spectrometry (MC-ICP-MS).* J. Anal. At. Spectrom., 2001. **16**(12): p. 1389-1392.
44. Jakubowski, N., T. Prohaska, L. Rottmann, and F. Vanhaecke, *Inductively coupled plasma- and glow discharge plasma-sector field mass spectrometry: Part I. Tutorial: Fundamentals and instrumentation.* J. Anal. At. Spectrom., 2011. **26**(4): p. 693-726.
45. Catanzaro, E.J., T.J. Murphy, G.E. L., and S.W. R, *Absolute Isotopic Abundance Ratio and Atomic Weight of Terrestrial Rubidium. Journal of Research of the National Bureau of Standards*, 1969. **73A**(511).

46. de Laeter, J.R., J.K. Böhlke, P. De Bièvre, H. Hidaka, H. Peiser, K. Rosman, and P. Taylor, *Atomic weights of the elements. Review 2000 (IUPAC Technical Report).* Pure Appl. Chem., 2003. **75**(6): p. 683-800.
47. Horsky, M., J. Irrgeher, and T. Prohaska, *Evaluation strategies and uncertainty calculation of isotope amount ratios measured by MC ICP-MS on the example of Sr.* Anal. Bioanal. Chem., 2016 **408**(2).
48. Fietzke, J., V. Liebetrau, D. Günther, K. Gürs, K. Hametner, K. Zumholz, T.H. Hansteen, and A. Eisenhauer, *An alternative data acquisition and evaluation strategy for improved isotope ratio precision using LA-MC-ICP-MS applied to stable and radiogenic strontium isotopes in carbonates.* J. Anal. At. Spectrom., 2008. **23**(7): p. 955-961.
49. Halicz, L., I. Segal, N. Fruchter, M. Stein, and B. Lazar, *Strontium stable isotopes fractionate in the soil environments?* Earth. Planet. Sci. Lett., 2008. **272**(1-2): p. 406-411.
50. Waight, T., J. Baker, and D. Peate, *Sr isotope ratio measurements by double-focusing MC-ICPMS: Techniques, observations and pitfalls.* Int. J. Mass spectrom., 2002. **221**(3): p. 229-244.
51. Krabbenhöft, A., J. Fietzke, A. Eisenhauer, V. Liebetrau, F. Böhm, and H. Vollstaedt, *Determination of radiogenic and stable strontium isotope ratios (87Sr/86Sr; δ88/86Sr) by thermal ionization mass spectrometry applying an 87Sr/84Sr double spike.* J. Anal. At. Spectrom., 2009. **24**(9): p. 1267-1271.
52. Moore, L.J., T.J. Murphy, I.L. Barnes, and P.J. Paulsen, *Absolute Isotopic Abundance Ratios and Atomic Weight of a Reference Sample of Strontium.* Journal of Research of the National Bureau of Standards, 1982. **87**(1): p. 1-8.
53. Nier, A.O., *The isotopic constitution of strontium, barium, bismuth, thallium and mercury.* Physical Review, 1938. **54**(4): p. 275.
54. Liu, H.C., C.F. You, K.F. Huang, and C.H. Chung, *Precise determination of triple Sr isotopes (δ87Sr and δ88Sr) using MC-ICP-MS.* Talanta, 2012. **88**: p. 338-344.
55. Revel-Rolland, M., P. De Deckker, B. Delmonte, P.P. Hesse, J.W. Magee, I. Basile-Doelsch, F. Grousset, and D. Bosch, *Eastern Australia: A possible source of dust in East Antarctica interglacial ice.* Earth. Planet. Sci. Lett., 2006. **249**: p. 1-13.
56. Balcaen, L., I. De Schrijver, L. Moens, and F. Vanhaecke, *Determination of the Sr-87/Sr-86 isotope ratio in USGS silicate reference materials by multi-collector ICP-mass spectrometry.* Int. J. Mass spectrom., 2005. **242**(2-3): p. 251-255.
57. Faure, G. and T. Mensing, *Isotopes: Principles and Applications*. 2005, Wiley: Hoboken, NJ, USA.
58. Yang, L., C. Peter, U. Panne, and R.E. Sturgeon, *Use of Zr for mass bias correction in strontium isotope ratio determinations using MC-ICP-MS.* J. Anal. At. Spectrom., 2008. **23**(9): p. 1269-1274.
59. Nomura, M., K. Kogure, and M. Okamoto, *Isotopic abundance ratios and atomic weight of zirconium.* International Journal of Mass Spectrometry and Ion Physics, 1983. **50**(1): p. 219-227.
60. Ohno, T., T. Komiya, Y. Ueno, T. Hirata, and S. Maruyama, *Determination of Sr-88/Sr-86 mass-dependent isotopic and radiogenic isotope variation of Sr-87/Sr-86 in the Neoproterozoic Doushantuo Formation.* Gondwana Res., 2008. **14**(1-2): p. 126-133.
61. Hirata, T. and T. Yamaguchi, *Isotopic analysis of zirconium using enhanced sensitivity-laser ablation-multiple collector-inductively coupled plasma mass spectrometry.* J. Anal. At. Spectrom., 1999. **14**(9): p. 1455-1459.
62. Sahoo, S.K. and A. Masuda, *Precise measurement of zirconium isotopes by thermal ionization mass spectrometry.* Chem. Geol., 1997. **141**(1-2): p. 117-126.
63. Nebel, O., K. Mezger, E.E. Scherer, and C. Münker, *High precision determinations of 87Rb/85Rb in geologic materials by MC-ICP-MS.* Int. J. Mass spectrom., 2005. **246**(1-3): p. 10-18.

64. Münker, C., S. Weyer, E. Scherer, and K. Mezger, *Separation of high field strength elements (Nb, Ta, Zr, Hf) and Lu from rock samples for MC-ICPMS measurements.* Geochem. Geophys. Geosyst., 2001. **2**(12).
65. Woodhead, J., *A simple method for obtaining highly accurate Pb isotope data by MC-ICP-MS.* J. Anal. At. Spectrom., 2002. **17**(10): p. 1381-1385.
66. Baxter, D.C., I. Rodushkin, E. Engström, and D. Malinovsky, *Revised exponential model for mass bias correction using an internal standard for isotope abundance ratio measurements by multi-collector inductively coupled plasma mass spectrometry.* J. Anal. At. Spectrom., 2006. **21**(4): p. 427-430.
67. JCGM100:2008, *Evaluation of measurement data — Guide to the expression of uncertainty in measurement*, J.C.f.G.i.M.-. ISO, Editor. 2012.
68. Kragten, J., *Tutorial review. Calculating standard deviations and confidence intervals with a universally applicable spreadsheet technique.* Analyst, 1994. **119**(10): p. 2161-2165.
69. Berglund, M. and M.E. Wieser, *Isotopic compositions of the elements 2009 (IUPAC technical report).* Pure Appl. Chem., 2011. **83**(2): p. 397-410.